ORNL/TM-11238

OAK RIDGE
NATIONAL
LABORATORY

MARTIN MARIETTA

Study and Development of Advanced Control Techniques for Nuclear Reactors and Robots

Carlos March-Leuba

OPERATED BY
MARTIN MARIETTA ENERGY SYSTEMS, INC.
FOR THE UNITED STATES
DEPARTMENT OF ENERGY

ORNL/TM-11238

Instrumentation and Controls Division

STUDY AND DEVELOPMENT OF ADVANCED CONTROL TECHNIQUES FOR NUCLEAR REACTORS AND ROBOTS*

Carlos March-Leuba

Date Published: August 1989

*Dissertation presented for the Doctor of Philosophy Degree,
The University of Tennessee, Knoxville

Prepared by the
OAK RIDGE NATIONAL LABORATORY
Oak Ridge, Tennessee 37831
MARTIN MARIETTA ENERGY SYSTEMS, INC.
for the
U.S. DEPARTMENT OF ENERGY
under Contract No. DE-AC05-84OR21400

TABLE OF CONTENTS

TABLE OF CONTENTS (continued)

TABLE OF CONTENTS (continued)

LIST OF FIGURES

LIST OF FIGURES (continued)

FIGURE PAGE

ABSTRACT

This report studies and develops some aspects of the optimal control theory with the objective of evaluating benefits that the nuclear industry could obtain by applying advanced control techniques.

First, the basic relationship between optimal control theory and closed-loop control design has been identified. As a result of this work, new algorithms have been developed for feedback implementations. The applicability of these new algorithms to problems such as state estimation, filtering, model update, and model decoupling has been studied. In addition, new alternatives to control design that are not based on optimal control theory have been developed.

A broad range of application examples has been presented for several physical systems, including pressurized water nuclear reactors, boiling water nuclear reactors, steam generators, and robotics.

1. INTRODUCTION

The instrumentation and control hardware for nuclear reactors has been developed based primarily on analog circuits, because digital instrumentation was not available when most nuclear reactors were built. Control algorithms were designed to take into account the analog constraints, so that an impressive amount of creative effort had to be devoted to the design of the analog controllers. Given the limited tools available to the designer, the results obtained were excellent, as the performance of these control algorithms has demonstrated for a long period of time.

Analog circuits are becoming obsolete; they are not the standard hardware used by the control systems industry anymore. Indeed, major vendors of control hardware in the United States are not selling replacement analog systems or even spare parts for existing systems. Thus, the nuclear industry is now facing the challenge of having to move to digital-based hardware systems.

Certainly, it is necessary to change the hardware, but the question that remains is: Do we also have to change the control algorithms?

The introduction of fast and reliable microprocessors has opened the possibility of performing sophisticated on-line calculations. With the new tools available, it appears to be possible to improve the dynamic behavior of nuclear reactors. Perhaps, by using more sophisticated control algorithms, nuclear reactors could be operated under more demanding conditions, or perhaps it will be possible to decrease costly downtime.

This report assesses and develops these possibilities.

1.1 MOTIVATION AND OBJECTIVES

In the past three decades significant advances in control techniques have been introduced in many engineering fields. In particular, aerospace engineering has been very innovative in developing algorithms that emphasize the characteristics of adaptability and robustness in the control of nonlinear systems. On the other hand, mathematicians have introduced new powerful tools to analyze and study the dynamic behavior of sophisticated systems.

A few of these advanced techniques have reached the nuclear engineering field. In the last few years, an important amount of research time has been invested in analyzing how much improvement can be achieved by applying advanced control algorithms to nuclear reactors. This report intends to be a contribution to that effort.

The objectives of this report are to:

1. assess optimal control theory as a tool for the development of closed-loop control algorithms;

2. develop alternative formulations of the optimal control theory for nonlinear systems suitable for on-line computer implementation;

3. study the applicability of the above alternative formulations to plant-state estimation, filtering, model updating, and large-model decomposition and decoupling;

4. implement the new techniques on a broad range of typical applications; and

5. develop new alternatives to control design that are not based on optimal control theory.

1.2 BACKGROUND

The two most important control hardware vendors in the United States (Foxboro and Baley) have discontinued the production of analog devices. Since the industry is having difficulties maintaining the existing systems, there is an ongoing effort to replace analog with digital controllers.

The benefits of the new digital control devices over analog systems are expected to be: (1) easier implementation, (2) better display of information for the operator, and (3) easier maintenance.

Yet, control strategies have not followed this renovative process. The algorithms implemented in the digital devices remain the same as those used in the analog systems. The main reason for conserving the old algorithms is that, in general, they appear to work well and, more importantly, they are well understood.

Unfortunately, the above statement is not always true. The good safety record of the nuclear industry seems to be related more to the intrinsic stability of nuclear reactors than to the performance of their control algorithms.

For instance, the level control of steam generators at low power is generally transferred to manual operation because the present automatic control system becomes unstable and causes reactor trips due to primary system overcooling. Similarly, boiling water reactors (BWRs) are primarily used as base-load reactors because the control design cannot handle fast load changes.

Since an increasing demand for better performing algorithms is expected in the next few years, there is a general interest in developing control algorithms that are able to perform over a wide range of operating conditions to avoid reactor trips. Thus, it is reasonable to predict that an investment in advanced control techniques will pay off by a reduction of expensive downtime and increased availability.

Control design can be classified into two major areas: closed-loop and open-loop designs. Closed-loop strategies introduce the control algorithm as a feedback to the system. Open-loop strategies are obtained off-line and then applied to the system. Both can be very powerful, and it is important to understand their advantages and disadvantages.

Open-loop controls allow one to introduce sophisticated calculations that, in principle, can lead the system to optimal performance. Unfortunately, these calculations have to be performed based on an approximate model of the plant. If the plant behavior is perturbed, the results are not optimal; in some cases, results can be catastrophic.

Feedback controllers are a dynamic part of the system and have the ability to adapt to unexpected perturbations. Stability can be predicted if no fundamental changes in dynamic behavior occur. The disadvantage is that feedback controllers can use only past information from the plant; they will not take into account future events or expected demands, which are known in many cases.

The research on advanced control techniques for nuclear reactors started in the 1960s with the work of Rosztoczy.[1] This author applied the recently published work of Pontryagin,[2] the Maximum Principle, to optimize control rod movement during transients in a simplified nonlinear nuclear core model. An analog computer was developed to solve the associated two-point boundary value problem. A more global study of the optimal control techniques and their applicability to nuclear reactors was done later by Mohler and Shen.[3] In Europe, advanced controllers were designed and applied to nuclear reactors in the late 1970s.[4]

In past years, some isolated work has been performed in the United States. Now, a more coordinated effort is being made through the Advanced Controls Program (ACTO)[5] at the Oak Ridge National Laboratory. This program represents a unique opportunity to study and analyze the benefits of advanced algorithms for the nuclear industry. This centralized and unified effort will allow to be conducted cutting edge research that cannot be afforded by any particular group alone. The ACTO program can be the breakthrough point for the nuclear industry in the United States. Huge benefits can be obtained on safety and improved operative capabilities.

1.3 PREVIEW OF REPORT

This report is organized as follows:

Section 2 is devoted to the study of optimal control-based feedback controllers. The purpose of this work is to show, by stepping through a series of examples, how the basic cost function minimization problem must be reformulated to obtain a closed-loop control strategy. Applications of closed-loop optimal control design proposed are: state estimation, parameter tracking, uncertainty tracking, and system decomposition.

Section 3 presents a new formulation of a class of nonlinear optimal control problems in which system parameters change arbitrarily with time. A variational technique based on Pontryagin's Maximum Principle (PMP) is used to track the time-varying parameters of the system and to calculate the optimal control action. An application to a nonlinear nuclear reactor in which feedback coefficients and sensors time constants are varying is presented.

Section 4 presents a new formulation of a class of nonlinear optimal control problems in which the measured signals are noisy and some system parameters change arbitrarily with time. The methodology is validated by an application to a nonlinear nuclear reactor model. The reformulation of the variational technique as an initial value problem allows this microprocessor-based algorithm to perform on-line filtering, parameter tracking, and control.

Section 5 shows some applications of the techniques presented to reactor monitoring problems. First, a transient reactivity monitor is presented that was tested and validated with a dynamic model of the Advanced Neutron Source (ANS) reactor. Second, a state monitor for a pressurized water reactor (PWR) is presented that is able to estimate the state variables of the system by analyzing noise-corrupted signals from the plant. Both applications use techniques presented in previous chapters.

Section 6 presents a comparison between the behavior of a BWR controlled with a standard proportional-integral (PI) controller and one controlled with a microprocessor-based optimal control algorithm. Both control algorithms are designed to make the BWR perform as a demand-following reactor. It is shown how the PI controller fails to keep the system stable at low flow, while the optimal nonlinear control is able to keep the stability of the system at any flow, thus, improving the transient behavior.

Section 7 presents an adaptive optimal control algorithm for uncertain nonlinear systems (for which the model is not completely known). It represents a novel approach to the problem of decoupling a large system from a set of simplified subsystems. A variational technique based on Pontryagin's Maximum Principle is used to track the system's unknown terms, decouple the subsystem models, and calculate the optimal control. To validate the algorithm, a system representing a two-link mechanical manipulator is simulated. In the control model, the coupling and friction terms are unknown. The robot's tasks are to follow a prescribed trajectory and to pick up an unknown mass. The inverse kinematics problem for the trajectory prescription in generalized coordinates is also solved by applying variational techniques.

Section 8 presents an application of the Hamilton-Jacobi approach, presented in Sect. 2, to the mechanical manipulator problem.

Section 9 presents a new algorithm to control steam generator water levels that does not rely on feedwater flow measurements. At low power, the feedwater signal is biased; therefore, the classical three-element controller fails and forces the transfer to manual control to avoid a reactor trip due to unstable conditions in the steam generator. Manual operation has been shown not to be very effective; in fact, a large number of reactor trips occur under these conditions. The algorithm documented in this section is able to compensate for the shrink and swell phenomenon by modulating the level set point according to differential changes on the pressure signals. In this way, it is possible to keep a strong and dynamic automatic level controller from 0 to 100% power.

Finally, Sect. 10 summarizes the conclusions of this report.

1.4 ORIGINAL CONTRIBUTIONS

The original contributions presented are:

1. the analysis of optimal control theory from the stability point of view and a study of the differences between open-loop and closed-loop implementation;

2. development of two new algorithms (the adjoint technique and the adaptive linear control of nonlinear systems technique) that can be applied to nonlinear systems (based on optimal control theory and leading to closed-loop designs);

3. the application of optimal control theory to parameter tracking, uncertainty tracking, model update, subsystem decoupling and decomposition, state estimation, and filtering;

4. a new approach based on optimal control theory to the inverse kinematic problem of the mechanical manipulators;

5. an alternative approach to the steam generator water level control problem;

6. performance of an extensive computer validation of the proposed algorithms, including applications to PWRs, ANS, BWRs, steam generators, and mechanical manipulators.

2. CLOSED-LOOP OPTIMAL CONTROL

The earliest documented closed-loop control design was developed by Ktesibios in Alexandria in the third century BC. He built a water clock based on a constant flow from a regulating tank to a clock tank. The level in the clock tank indicated the time. To keep the water level in the regulating tank constant, Ktesibios introduced the first known float valve to control the flow of water from the main source. A float valve acts as a feedback (closed-loop) control. If the water level goes down, it opens. If the level goes up, it closes. In spite of the simplicity of this design, it is extremely efficient. It seems almost impossible to design an equivalent open-loop control.

Modern control theory is based on the mathematical analysis of dynamic systems. Closed-loop controllers are generally designed by analyzing the stability of the system via linear or nonlinear stability theory. In this section we study how variational techniques can help in this design.

The calculus of variations was initiated by the Bernoulli brothers in the 17th century with the study of the brachistochrone problem. Since then it has become a powerful tool in almost all scientific domains, but the application of variational techniques to control design is a relatively recent development. The optimal control theory was introduced independently by Pontryagin and Bellman in the 1960s.

The basic optimal control theory leads to open-loop implementations. Unfortunately, dynamic systems are subject to random perturbations; therefore, closed-loop formulations are more robust because they can adjust to unanticipated events.

2.1 OPTIMAL CONTROL

This section formulates a continuous-time optimal control problem and develops the associated Pontryagin's Maximum Principle. Many books and articles have been published on this subject since the original work of Pontryagin. This section follows the formulation presented by Luenberger.[6]

2.1.1 General Structure of an Optimal Control Problem

The basic optimal control problem is defined by:

1. a dynamic system (plant) for which input functions can be specified (controls), and

2. a cost function whose value depends on the system's dynamic behavior and, in some sense, defines and measures the quality of that behavior.

For example, the dynamic system might be a nuclear reactor core with an input function corresponding to the reactivity rod control. The cost function can then be defined as the error between the actual neutron density and the set point for the reactor.

The optimal control theory goal is to determine which are the input functions that minimize the value of the cost function. In our example, the goal would be to obtain a control rod reactivity strategy that minimizes the error between the set point for the reactor and the actual neutron density.

2.1.2 The Maximum Principle

The publication by Pontryagin of his Maximum Principle has been one of the most important events in the development of the control theory. Pontryagin applied the calculus of variations to the problem of finding the input functions that maximize (or minimize) the cost function.

Given a dynamic system,

$$dx/dt = f(x,u) \quad , \tag{2-1}$$

where x represents the state variable, u the input function (control), and a cost function (to be minimized) is defined as

$$J = \int_0^{tf} V(x,u)\ dt \quad . \tag{2-2}$$

Pontryagin's Maximum Principle can be stated as follows:

Theorem (Maximum Principle). Suppose $u(t) \epsilon U$ and $x(t)$ represent the optimal control and state trajectory for the optimal control problem. Then there is an adjoint trajectory $w(t)$ such that $u(t)$, $x(t)$, and $w(t)$ together satisfy

$$dx/dt = f(x,u) \quad \text{(system)} \quad ; \tag{2-3a}$$

$$x(0) = x_o \quad \text{(state condition)} \quad ; \tag{2-3b}$$

$$-\,dw^T/dt = H_x(w,x,u) \quad \text{(adjoint)} \quad ; \tag{2-3c}$$

$$w(tf) = 0 \quad \text{(adjoint final condition)} \quad ; \tag{2-3d}$$

and for all t and all $v \in U$,

$$H(w,x,v) < H(w,x,u) \ \text{(maximum condition)} \tag{2-3e}$$

where H is the Hamiltonian

$$H(w,x,u) = w^T f(x,u) + V(x,u) \quad . \tag{2-3f}$$

Condition (2-3e), the maximum condition, means that the derivatives of H with respect to each component of u must vanish, and, if the objective is to minimize the cost function, then condition (2-3e) must be interpreted as a minimum condition. A detailed proof of this theorem can be found in ref. 2.

2.2 CLOSED-LOOP OPTIMAL CONTROL: LINEAR SYSTEMS

Control designers feel comfortable with closed-loop implementations; that is, the algorithm obtains the input function (control) as a function of the state variables of the system. The reason is clear, since under these conditions the stability of the control algorithm can be studied and predicted.

2.2.1 The Regulator Problem

To simplify notation and make this section easier to understand, we will use a one-dimensional example.

Let us assume that the system we want to control can be represented by the differential equation,

$$dx/dt = ax + u \quad , \qquad (2\text{-}4)$$

where x is the state variable and u is the control. This system has an equilibrium at $x = 0$ and $u = 0$.

Our goal is to regulate this system around its equilibrium, that is, to design a control algorithm that, if the system equilibrium is perturbed, will place the system back in the equilibrium position. This goal can be represented by defining the function $V(x,u)$ as

$$V(x,u) = 1/2\ x^2Q + 1/2\ u^2R \quad , \qquad (2\text{-}5)$$

where Q and R are weights.

Now we can apply the Maximum Principle. First we construct the Hamiltonian,

$$H(x,w,u) = w(ax+u) + 1/2\ x^2Q + 1/2\ u^2R \quad , \qquad (2\text{-}6)$$

the adjoint equation ($-dw/dt = H_x$) is given by

$$dw/dt = -aw - xQ \quad , \qquad (2\text{-}7)$$

and u is obtained by demanding $H_u = 0$, which results in

$$u = -w/R \quad . \qquad (2\text{-}8)$$

Substituting Eq. (2-8) into the model, we obtain this set of equations:

$$dx/dt = ax - w/R \quad ; \qquad (2\text{-}9a)$$

$$dw/dt = -aw - xQ \quad . \tag{2-9b}$$

Equation (2-9) represents the system's dynamic behavior under the action of the optimal control.

Let us now assume that the system has been perturbed from equilibrium. We want to know whether both equations together [Eqs. (2-9a) and (2-9b)] are stable, that is, whether they return the system to equilibrium following a small perturbation.

We have chosen a linear example because its stability is easier to study. First, we realize that $x = 0$ and $w = 0$ is still an equilibrium point because it makes the derivatives zero. Then, we have to analyze whether the eigenvalues of the system have negative real parts. The characteristic equation of this system can be written as

$$s^2 - a^2 - Q/R = 0 \ .$$

Since Q and R are positive, there is always a positive eigenvalue; therefore, an asymptotically stable equilibrium state cannot be reached in general.

This example gives a heuristic understanding of why optimal control techniques are not suitable for feedback (closed-loop) applications. We can only expect to find a good initial condition for adjoint $w(0)$ that will place the system in the target state at a given final time. But, because of the intrinsic instability, we cannot expect to keep the system in that target state.

2.2.2 The Linear-Quadratic Algorithm

The linear-quadratic (LQ) algorithm was developed by Kalman,[7] and it has been widely used by the control designers mainly because it allows closed-loop implementations. LQ can be applied only to problems in which the dynamic system is linear and the cost function is quadratic. In this section the basic formulation of the problem is studied and analyzed.

2.2.2.1 The LQ Algorithm

The LQ algorithm is based on the idea that, since the system represented by Eq. (2-9) is linear, both $x(t)$ and $w(t)$ depend linearly on x_o; therefore, $w(t)$ should depend linearly on $x(t)$. Accordingly, we try a solution for Eq. (2-9) of the form,

$$w(t) = P(t)x(t) \quad , \tag{2-10}$$

where $P(t)$ represents the linear relation between the state and the adjoint variables. Taking the derivative of Eq. (2-10) and introducing the result in Eq. (2-9), we obtain the condition,

$$0 = [dP(t)/dt + 2aP(t) - P^2(t)/R + Q]x(t) \quad , \tag{2-11}$$

which will be satisfied for any $x(t)$ if $P(t)$ is chosen as a solution of the Riccati equation,

$$-dP/dt = 2aP - P^2/R + Q \quad . \tag{2-12}$$

From the boundary condition $w(tf) = 0$, we derive $P(tf) = 0$, a final condition. We must, however, solve this equation by integrating backwards in time from $t = tf$.

2.2.2.2 The Feedback Solution

Now, considering tf very large, we can assume that Eq. (2-12) may have reached an equilibrium near $t = 0$ (we recall that here time is incremented backwards). Thus, $P(t)$ may be approximated by its equilibrium value, P. Under this approximation and from Eq. (2-8) we obtain

$$u(t) = -(P/R)x \quad , \tag{2-13}$$

which gives the control input with a time-invariant feedback structure. With this approximation, the optimal system is dynamically represented by

$$dx/dt = ax - (P/R)x \quad . \tag{2-14}$$

Let us analyze the steady state solutions of the Ricatti equation. From Eq. (2-12) we obtain

$$P = R[a \pm (a^2 + Q/R)^{½}] \quad , \tag{2-15}$$

which leads to a dynamic system,

$$dx/dt = [\pm(a^2 + Q/R)^{½}]x \quad . \tag{2-16}$$

Equation (2-15) has two solutions. By choosing the value of P that leads to a negative eigenvalue, we obtain a stable closed-loop formulation.

By numerical calculations, we have checked that the stable solution corresponds to the value of P obtained by integrating backwards Eq. (2-12) with final condition $P(t_f) = 0$. But the LQ approach will lead only to a stable closed-loop implementation if we keep P constant all the time. In fact, if we try to solve Eq. (2-12) forward in time, the system again becomes unstable.

2.2.2.3 The Dual LQ Algorithm

It is interesting to note that the steady state Riccati algebraic equation not only represents the equilibrium points of Eq. (2-12), but also the equilibrium points of the time-reversed equation,

$$dP/dt = 2aP - P^2/R + Q \quad , \tag{2-17}$$

which can be derived from the dual system,

$$dx/dt = -ax + w/R \quad ; \tag{2-18.a}$$

$$dw/dt = \quad aw + xQ \quad . \tag{2-18.b}$$

The dual system is obtained by integrating backwards in time the cost function, or more easily, by applying two transformations: map t into $-t$, and then map $-t$ into $-t + t_f$.

Equation (2-17) must be solved forward in time and with initial condition $P(0) = 0$, and it reaches the steady state solution that makes the system stable. The simultaneous solution of Eqs. (2-14) and (2-17) forward in time leads to a stable system with a closed-loop control.

2.2.3 The Hamilton-Jacobi Equation

Let us now study the dynamic behavior of the cost function. First we define a dynamic cost function as

$$J(t) = \int_0^t V(x,u)\, d\tau \quad . \tag{2-19}$$

Taking the total derivative of $J(t)$ with respect to t,

$$J_t = -[\, J_x dx/dt - V(x,u)] \quad , \tag{2-20}$$

and defining the Hamiltonian as

$$H(J_x,x,u) = J_x dx/dt - V(x,u) \quad , \tag{2-21}$$

we obtain

$$J_t = -H(J_x,x,u) \quad . \tag{2-22}$$

Equation (2-22) is known as the Hamilton-Jacobi equation in classical mechanics. To minimize the temporal evolution of $J(t)$, we have to select u (the control) such that it both minimizes the Hamiltonian and keeps the value of the Hamiltonian constant and equal to zero during the evolution of the system.

Returning to the linear example used before, we first construct the Hamiltonian as

$$H = J_x(ax+u) - 1/2\ x^2 Q - 1/2\ u^2 R \quad . \tag{2-23}$$

Second, we choose u such that it minimizes H; that is,

$$H_u = 0 \quad ,$$

$$u = J_x/R \quad . \tag{2-24}$$

Finally, we substitute Eq. (2-24) in Eq. (2-23) and demand that $H = 0$.

$$0 = J_x ax + 1/2\ (J_x)^2/R - 1/2\ x^2 Q \quad . \tag{2-25}$$

Assuming now that the solution of this partial differential equation is of the form,

$$J = -1/2\ Px^2 \quad , \tag{2-26}$$

it follows that

$$x^2(-2aP + P^2/R - Q) = 0 \quad . \tag{2-27}$$

Equation (2-27) leads to a solution that is equivalent to the *LQ* algorithm. Given a state, x, Eq. (2-24) returns the optimal control that should be applied to the system. We have not specified a final time; therefore, this optimal closed-loop formulation of the control problem will be asymptotically stable.

It is important to note that the right-hand side of Eq. (2-26) is the first term of the Taylor series expansion of the solution. In this linear example with a quadratic cost function, the second term of the expansion leads to the exact solution of the problem (note that second order in J means first order in the expansion of the partial of J with respect to x). In general, it will be necessary to add more terms to the expansion to solve nonlinear problems.

2.3 CLOSED-LOOP OPTIMAL CONTROL: NONLINEAR SYSTEMS

Models of realistic systems are seldom linear. Unfortunately, it is always more difficult to deal with nonlinear models, and the simplicity in the control design is lost. In this section we will present some techniques to solve nonlinear control problems. Again, our goal is to be able to design a stable closed-loop control. It will be seen that there is not a general algorithm to solve the problem. For each control case, the control designer will have to exercise his own creativity.

As shown in the previous section, the most clear and meaningful way of dealing with optimal control problems is the Hamilton-Jacobi equation. In many cases it will be necessary to solve this equation by expanding the solution in a Taylor series. In general, this will lead to an almost impossible analytic task. We are going to show how in some cases this work can be simplified by redefining the cost function. There will not be a general rule for doing this, and here is where the control designer will have a major role to play. Again, to simplify notation and make this section easier to understand, we will use an example.

2.3.1 The Hamilton-Jacobi Equation

Let us suppose that we want to design a control algorithm for the following nonlinear problem,

$$dx/dt = ax^2 + u \quad . \tag{2-28}$$

First we realize that the linearization technique will fail. If this model is linearized around $x = 0$, all the information about the dynamics of the system is lost; therefore, it is necessary to deal directly with the nonlinear model.

2.3.1.1 Cost Function Transformation Approach

If we now write the cost function in the standard quadratic form (see linear example), the solution of the Hamilton-Jacobi equation will demand more than one term in the Taylor series expansion. To see if we are able to rewrite the cost function in a way that simplifies the solution, we try:

$$V(x,u) = 1/2\ x^2Q + 1/2\ (u + ax^2)^2R \quad . \tag{2-29}$$

The related Hamiltonian [see Eq. (2-23)] will be

$$H = w(ax^2 + u) - 1/2\ x^2Q - 1/2\ (u + ax^2)^2R \quad , \tag{2-30}$$

where for simplicity we use the notation $w = J_x$. We choose u such that this Hamiltonian is minimized; that is, $H_u = 0$. Therefore,

$$u = w/R - ax^2 \quad . \tag{2-31}$$

Introducing Eq. (2-31) into Eq. (2-30) and demanding that $H = 0$, we get

$$0 = w^2/2R - 1/2\ x^2Q \quad . \tag{2-32}$$

Let us try a solution of the form

$$w = Px \quad , \tag{2-33}$$

which leads to

$$0 = (P^2/R - Q)x^2 \quad . \tag{2-34}$$

We have found a solution for P that is independent of x; therefore, we can develop a closed-loop implementation in this case of

$$u = -ax^2 - (Q/R)^{½}x/R \quad , \tag{2-35}$$

and

$$dx/dt = -(Q/R)^{½}x/R \quad . \tag{2-36}$$

Because Q and R are defined to be positive, this will always be a stable closed-loop implementation.

This example shows how a transformation in the cost function can simplify the analytical calculations and lead to a solution.

2.3.1.2 Direct Solution by Series Expansion

Because of the simplicity of this example, we can now try to solve it directly by applying a second-order expansion. This process will give us some idea of how difficult the problem can be.

First, we write again the cost function, but this time we use the standard form,

$$V(x,u) = 1/2\ x^2Q + 1/2\ u^2R \quad . \tag{2-37}$$

The Hamiltonian will be

$$H = w(ax^2 + u) - 1/2\ x^2Q - 1/2\ u^2R \quad . \tag{2-38}$$

$H_u = 0$ and $H = 0$ lead to

$$u = w/R \tag{2-39}$$

and

$$0 = wax + w^2/2R - 1/2\ x^2Q \quad . \tag{2-40}$$

We now try a second-order expansion,

$$w = Px + Zx^2 \quad . \tag{2-41}$$

Introducing Eq. (2-41) into Eq. (2-40) and simplifying gets

$$0 = (P^2/R - Q)x^2 \quad , \tag{2-42}$$

$$0 = (a + Z/R)Px^3 \quad . \tag{2-43}$$

The coefficient of x^4 is not analyzed because it is expected to have contributions from higher expansion terms. The solutions for Eqs. (2-42) and (2-43) lead to

$$u = -ax^2 - (Q/R)^{1/2}/R \ , \tag{2-44}$$

which is equivalent to the solution that we get by minimizing the simplified cost function.

In this special case we can expect that higher order expansions will lead to the same solution; therefore, we can stop our study at the second order. But in general, it will be very difficult to decide where to stop.

2.3.2 Adaptive Linear Control of Nonlinear Systems

Sometimes dealing directly with nonlinear systems demands too much analytic work. In these cases, control designers are tempted to linearize the system and simplify the problem. In this section we present a technique to update the linearized control.

In Sect. 2.2.3, we have shown that dual LQ Eq. (2-17) leads to the steady state solution of the equation forward in time. We have seen that this solution is the one that gives stability in the closed-loop applications. We can use this property of the dual equation to obtain an adaptive linear control for a nonlinear system. Again, we use an example to show the methodology. It is important to know that this is a heuristic approach, and it will be difficult to guarantee the stability of the final design.

Returning to our nonlinear model, we linearize around x_o:

$$dx/dt = (ax_o)x + u \quad . \tag{2-45}$$

Note that this linearization is not a Taylor series expansion. It will be seen later that it works better. Again, the designer has to decide what to do.

Dual LQ Eq. (2-17) in this case will be

$$dP/dt = 2(ax_o)P - P^2/R + Q \quad , \tag{2-46}$$

and the optimal control is given by

$$u = -Px/R \quad . \tag{2-47}$$

The adaptive linear control algorithm can be achieved by updating the value of x_o:

$$dx/dt = ax^2 - Px/R \quad , \tag{2-48}$$

and

$$dP/dt = 2axP - P^2/R + Q \quad . \tag{2-49}$$

Let us see how this formulation works. The initial condition for Eq. (2-49) is the steady state value of P evaluated at the initial value of x. We can expect that if x is perturbed, Eq. (2-49) will evolve to the steady state solution again (updating the value of P).

We have checked by computer simulation that this particular case works. In order to perform an analytic study of this problem, we have to simplify it. Let us assume that Eq. (2-49) reaches the steady state fast enough to assume that the value of P is always the steady state solution. Then,

$$P = -axR - R[(ax)^2 + Q/R]^{\frac{1}{2}} \quad . \tag{2-50}$$

The system evolves with time as

$$dx/dt = - [(ax)^2 + Q/R]^{\frac{1}{2}}x \quad , \tag{2-51}$$

which is a stable solution.

2.3.3 The Dual Adjoint Technique

We have seen that applying the dual LQ equation to the system gets a stable closed-loop control. The dual equation is obtained by integrating the cost function backwards. We can interpret this as though we were applying the backward-in-time solution for the control problem to the forward-in-time model of the plant. This interpretation leads to the dual adjoint technique. In this case, we calculate the value of the control by integrating the adjoint backwards in time and applying the result to the forward-in-time system. Again, this is an intuitive approach, and we cannot find any reason to justify it. In fact, it will be shown that this methodology will work only if the system is stable.

Let us study the dual adjoint approach by applying it to the linear example. The model and the dual adjoint will be

$$dx/dt = ax - w/R \quad , \tag{2-52a}$$

$$dw/dt = aw + xQ \quad . \tag{2-52b}$$

The eigenvalues of this system are

$$s = a \pm i \, (Q/R)^{2} \quad . \tag{2-53}$$

Therefore, the dual adjoint technique leads to a stable implementation only if the system is stable.

Even if the system is stable, we cannot say that the solution will be optimal. In fact, this algorithm acts as a second-order filter with the break frequencies of the original system. If the break frequencies are negative, the filter will move the system back to equilibrium.

The main advantage of this technique is that, if it works, the control algorithm is extremely easy to design. This simplicity must be taken into account when we have a multiple-input multiple-output nonlinear problem for which solving the Hamilton-Jacobi equation directly can be extremely difficult.

2.4 APPLICATIONS

In this section, some applications of optimal control theory are presented. We will show what kind of cost functions need to be minimized in each case. The particular solution for the minimization problem will depend on the specific case, and any of the previously shown techniques could be used.

2.4.1 State Estimation: Filtering

In this section the optimal control methodology is applied to the problem of estimating the actual state of the plant from detector signals that are perturbed with additive noise.

We define

$$\mathbf{s} = \mathbf{y}_d + \boldsymbol{\eta} \qquad (2\text{-}54)$$

as the set of signals coming from the plant detectors, where $\mathbf{y}_d$ represents the detector state variables, and $\boldsymbol{\eta}$ represents an additive noise with zero mean.

We also define $\mathbf{x}$ as the estimated plant state. The dynamic estimation of $\mathbf{x}$ can be obtained from

$$d\mathbf{x}/dt = \mathbf{G}(\mathbf{x},\mathbf{u}) + \mathbf{v} \quad , \qquad (2\text{-}55)$$

where $\mathbf{G}$ is an approximated model of the plant (predictor) and $\mathbf{v}$ is the dynamic correction (corrector) that can be obtained by minimizing the cost function,

$$J_F = \int_0^{tf} \{[\mathbf{s}-\mathbf{x}_d]^T Q_f [\mathbf{s}-\mathbf{x}_d] + \mathbf{v}^T R_f \mathbf{v}\} dt \quad . \qquad (2\text{-}56)$$

2.4.2 Parameter Tracking

This section shows how the optimal control methodology can be used to update the plant time-varying parameters.

We assume that there is a set of parameters, $\mathbf{a}$, that can change arbitrarily with time. Our control model has to be updated on-line, otherwise, we cannot guarantee that the calculated control will be optimal. The updating of the control model can be achieved by applying again the optimal control techniques. In this case, we assume that the magnitude of $\mathbf{a}$ will minimize the cost function,

$$J_P = \int_0^{tf} \{[\mathbf{x}-\mathbf{m}]^T Q_p [\mathbf{x}-\mathbf{m}] + \mathbf{a}^T R_p \mathbf{a}\} dt \quad , \qquad (2\text{-}57)$$

where $\mathbf{m}$ represents the control model state variables.

2.4.3 Uncertainty Tracking

Models of realistic systems are seldom completely known. The variational techniques that we have presented can also be used to track the unknown (uncertain) part of the model.

The formulation is similar to the one for parameter tracking. We want to find which are the optimal values for the uncertainty, $\mathbf{p}$, that make the approximated model of the plant match the signals coming from the detectors; that is, we want to minimize the cost function,

$$J_U = \int_0^{tf} \{[\mathbf{x}-\mathbf{m}]^T Q_u [\mathbf{x}-\mathbf{m}] + \mathbf{p}^T \mathbf{R}_u \mathbf{p}\} dt \quad . \tag{2-58}$$

2.4.4 System Decomposition

Often the plant's dynamic model involves a large number of differential equations. In this case, it may be convenient to decompose the large model into a set of decoupled subsystems. The uncertainty tracking method can be used to achieve an efficient decomposition without losing too much information.

Let us assume that

$$d\mathbf{x}/dt = \mathbf{F}(\mathbf{x},\mathbf{u}) \tag{2-59}$$

represents the mathematical model of the plant that we wish to control, where vector $\mathbf{x}$ represents the n state variables and $\mathbf{u}$ represents the m controls. Let

$$d\mathbf{x}_i/dt = \mathbf{F}_i(\mathbf{x}_i,\mathbf{u}_i) + \mathbf{p}_i \ , \qquad i = 1,\ k \tag{2-60}$$

represent a set of k subsystems formulated in such a way that they are uncoupled. To guarantee that this set of subsystems represents the whole system, we introduce the unknown set of functions, $\mathbf{p}_i$, whose values at time t can be obtained by the optimal matching of the signals coming from the detectors, with the values for the state variables given by the numerical integration of the subsystem's mathematical models. Actually, this problem can be formulated as an optimal control problem. We want to know what the values are of controls (unknown function $\mathbf{p}$) that make the subsystems follow the demand (detector signals).

2.5 SUMMARY

In Sect. 2 we reviewed the applications of optimal control theory to feedback control design. It has been seen that Pontryagin's Maximum Principle leads to open-loop strategies. In some cases, a closed-loop implementation can be achieved by solving directly the so-called Hamilton-Jacobi equation. This approach is relatively easy to implement for linear cases. Unfortunately, more analytic work is necessary in the nonlinear case. Some simplification can be obtained in these cases by choosing an "ad hoc" cost function. In general, the solution of the Hamilton-Jacobi equation will be extremely difficult. In this section, some new alternative approaches have been presented. Finally, some of the many applications of closed-loop optimal control have been shown, such as filtering, model update and decomposition, and control.

3. OPTIMAL PARAMETER TRACKING AND CONTROL OF NONLINEAR SYSTEMS WITH TIME-VARYING PARAMETERS

The practical applications of Pontryagin's Maximum Principle-based control algorithms have been hindered by the fact that drastic simplifications must be done to obtain on-line solutions. For example, the LQ algorithm, the most popular and perhaps the only one that to date allows on-line solutions, requires the use of linearized models and assumes that the relation [Eq. (2-10)] between system and adjoint equations is time-independent. Unfortunately, these conditions do not apply to the most common case, a nonlinear system with time-varying parameters.

The ideal demand-following adaptive control should:

1. provide an optimal control philosophy;

2. provide parameter tracking so that the plant model reproduces the signals coming from the actual plant sensors at any time;

3. provide control flexibility, in the sense that the control limitations and possible failures are taken into account;

4. compensate for sensor delays and possible degradation; and

5. handle directly the nonlinear model, thus making it possible to apply the algorithm under any plant conditions.

In principle, all these requirements can be satisfied by applying PMP to a nonlinear model of the plant. The major practical problem arises in connection with the numerical solution of the resulting two-point boundary value problem (TPBVP).

The following sections present a new approach to the PMP formulation that allows on-line solutions by recasting the TPBVP into an initial value problem.

3.1 REFORMULATION OF THE OPTIMAL CONTROL PROBLEM

This section shows how the free terminal time (FTT) optimal control problem can be reformulated as the solution of differential equations with a set of initial conditions, instead of the classical TPBVP.

Let

$$dy/dt = F(\mathbf{y},\mathbf{u}) \tag{3-1}$$

be a nonlinear system, where $\mathbf{y}$ represents the state variables and $\mathbf{u}$ the controls. The FTT problem is formulated as the minimization of the extended cost function,

$$J = \int_{t0}^{tf} [H(\mathbf{y},\mathbf{w},\mathbf{u}) - \mathbf{w}^T d\mathbf{y}/dt]dt \quad , \tag{3-2}$$

where $\mathbf{w}$ is a set of Lagrange multipliers (adjoints or momenta), H represents the Hamiltonian, defined as $H = \mathbf{w}^T d\mathbf{y}/dt + V(\mathbf{y},\mathbf{u})$, and V can be interpreted as the potential that will force the system to move along the desired trajectory. We assume that H is time-invariant, $\mathbf{y}(t0)$ and $\mathbf{y}(tf)$ are given, and the system is in steady state at $t = t0$. Because of the symmetry of the problem, the minimization of the cost function can be done backwards. After a time inversion of the expression for J, and after performing the equivalent steps to the PMP, the following inverted Hamilton equations are obtained:

$$dy_i/dt = -dH/dw_i \quad , \tag{3-3}$$

$$dw_i/dt = dH/dy_i \quad , \tag{3-4}$$

and the conditions,

$$dH/du_i = 0 \quad , \tag{3-5}$$

$$(H)_{t0} = 0 \quad . \tag{3-6}$$

If steady state conditions are assumed at $t = t_0$, and dV/du_i is different from zero, then, the initial conditions for $\mathbf{w}$ can be found. Moreover, because the state variables are time-reversal invariant and the controls are only functions of $\mathbf{y}$ and $\mathbf{w}$, the first Hamiltonian equation can be solved forward instead of backwards, as the result of the variations implies. Then, under these special conditions, the FTT problem can be solved forward in time as the solution of differential equations with initial conditions. Notice that condition (3-6) will constrain the algorithm to demand-following or regulation problems, (the ones in which we are interested), and perhaps the only ones that need on-line solutions.

3.2 PARAMETER TRACKING AND CONTROL

As stated before, our goal is to develop an algorithm that must be able to update the model by tracking the time-varying parameters while it is calculating the optimal control.

Let

$$d\mathbf{y}/dt = F(\mathbf{y},t,\mathbf{b},\mathbf{a}',\mathbf{u}) \tag{3-7}$$

be a nonlinear system where $\mathbf{y}$ represents the state variables and signals from the plant, t the time, $\mathbf{b}$ the fixed parameters, $\mathbf{a}'$ the time-varying parameters, and $\mathbf{u}$ the controls.

Let

$$\mathbf{dx}/\mathrm{dt} = F(\mathbf{x},t,\mathbf{b},\mathbf{a}_0,\mathbf{u}) \quad (3\text{-}8)$$

be the system and detector model, where the $\mathbf{a}_0$ parameter set corresponds to a given steady state. The set of parameters $\mathbf{a}$ may vary with time, invalidating the optimal controls calculated using this model; thus, it is necessary to track the parameters. The approach taken in this work has been to realize that the time-varying parameters can be considered as the set $\mathbf{a}$ that minimizes the difference between $\mathbf{s}_y$ and $\mathbf{s}_x$ (where $\mathbf{s}$ means the subset of $\mathbf{y}$ or $\mathbf{x}$ representing the signals). Therefore, the parameters can be obtained by forcing the system to move through the potential V_p, defined as,

$$V_p = (\mathbf{s}_y-\mathbf{s}_x)^+Q(\mathbf{s}_y-\mathbf{s}_x) + (\mathbf{a}-\mathbf{a}_0)^+R(\mathbf{a}-\mathbf{a}_0) \quad , \quad (3\text{-}9)$$

where Q and R are weight matrices, $\mathbf{a}_0$ the steady-state parameter values, and $^+$ represents the transpose.

Following the algorithm developed in Sect. 3.1, we can now construct the Hamiltonian and obtain the inverted Hamilton equations for the momenta ($\mathbf{w}$) and the condition for the time-varying parameters:

$$H_p = \mathbf{w}^+\mathbf{dx}/dt + V_p \quad , \quad (3\text{-}10)$$

$$dw_i/dt = dH_p/dx_i \quad , \quad (3\text{-}11)$$

$$dH_p/da_i = 0 \quad . \quad (3\text{-}12)$$

Equations (3-11) and (3-8), in which $\mathbf{a}_0$ is updated with the $\mathbf{a}$ obtained from Eq. (3-12), represent a mathematical model of the system that is able to update the time-varying parameters during the transient. The initial conditions for $\mathbf{x}$ are known, and the initial conditions for $\mathbf{w}$ can be obtained assuming $V_p = 0$ and $\mathbf{dx}/dt = 0$ at $t = 0$. Notice that these assumptions support fundamental condition (3-6).

Now, the updated model can be controlled by forcing it to move under the potential, defined as

$$V_c = (\mathbf{d}-\mathbf{sd}_x)^+L(\mathbf{d}-\mathbf{sd}_x) + (\mathbf{u}-\mathbf{u}_0)^+M(\mathbf{u}-\mathbf{u}_0) \quad , \quad (3\text{-}13)$$

where $\mathbf{d}$ is a given demand for a state variables subset, $\mathbf{sd}_x$, and $\mathbf{u}_0$ is the steady state value for the controls. Again, following the formalism presented in Sect. 3.1, we can obtain the momenta and conditions associated with the control problem and, again assuming $V_c = 0$ at $t = 0$, the initial conditions.

3.3 APPLICATION TO A NONLINEAR NUCLEAR REACTOR

The algorithm presented in this report has been applied to a nonlinear reactor model. The plant was simulated with a four-dimensional model and three detectors. During the transient, the feedback coefficient due to the coolant temperature, the fuel temperature detector time constant, and coolant temperature detector time constant were time-dependent. The plant was forced to follow demands in neutron density and outlet coolant temperature by adjusting two control inputs: (1) reactivity, which was constrained to a given value, and (2) inlet coolant temperature.

The time-varying parameters were changing drastically during the transient, transforming the system's dynamics; therefore, it was necessary to track them. Figure 3.1 shows how the parameters that were obtained using our algorithm match the actual parameter values.

Figure 3.2 shows the controls that are necessary to follow the transient. Notice that the sinusoidal form of Fig. 3.2a is due to the sinusoidal change in coolant feedback coefficient. Figures 3.2a and 3.2b show how our algorithm allows both controls to interact: when u1 reaches the maximum, u2 carries all the work without discontinuities.

Figure 3.3 shows how demands in both neutron density and outlet coolant temperature were followed by the plant in spite of parameter changes and constraints in the controls.

Finally, Fig. 3.4 shows how the algorithm matches the actual values for (a) coolant and (b) fuel temperatures at any time by correcting for the delays introduced by the detection process.

3.4 SUMMARY

An optimal parameter tracking and control algorithm has been developed that allows us to find on-line solutions for demand-following problems for cases in which nonlinearities and time-varying parameters invalidated other known algorithms. A crucial result has been the recasting of Pontryagin's Maximum Principle technique for nonlinear systems as the solution of differential equations with initial conditions. The algorithm has been successfully applied to a nonlinear nuclear reactor model. Using the plant sensor signals, the parameters were updated during the transient, allowing the calculation of the optimal control strategy.

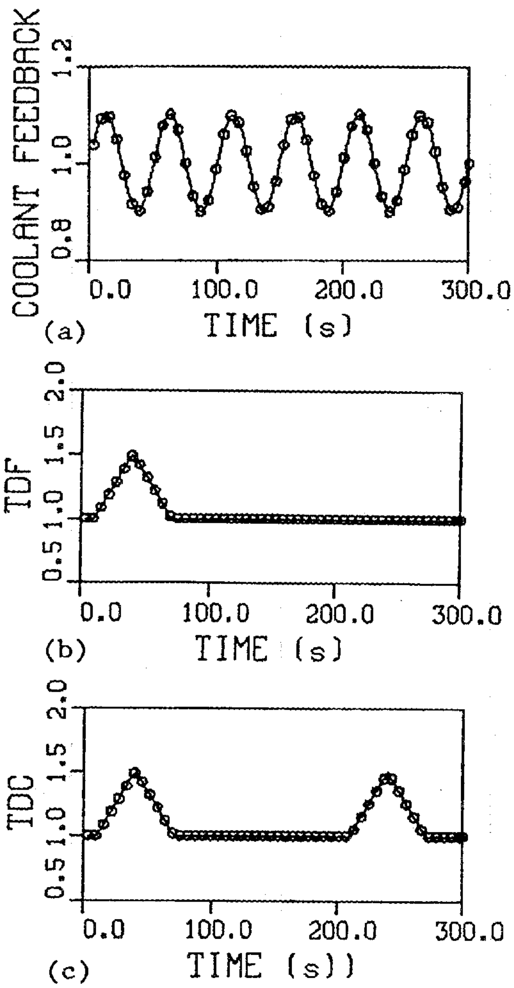

Fig. 3.1. Parameter tracking. Solid lines represent the actual values and circles the algorithm estimations: (a) coolant feedback coefficient, (b) coolant temperature detector time constant, and (c) fuel temperature time constant.

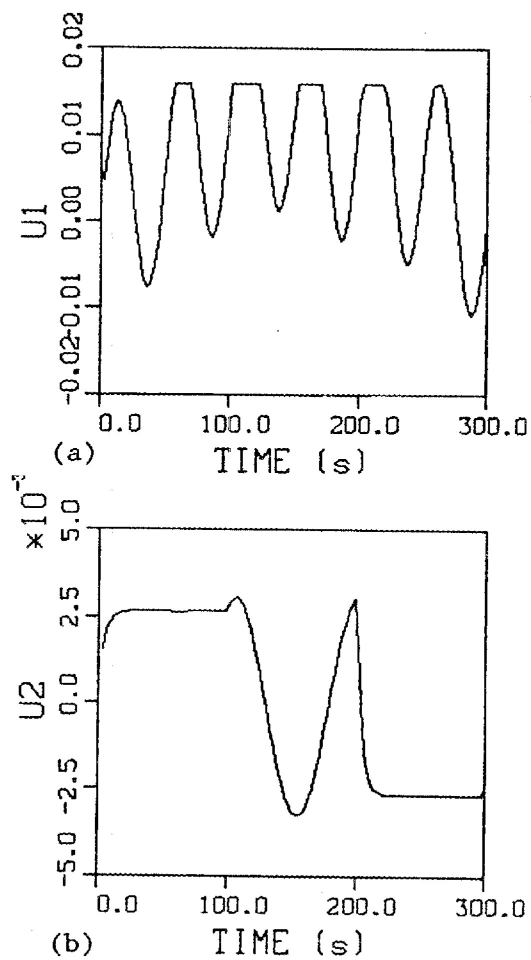

Fig. 3.2. Optimal controls: (a) *u*1, reactivity, which is constrained to *u*1 <0.016 (absolute units); and (b) *u*2, inlet coolant temperature (relative units).

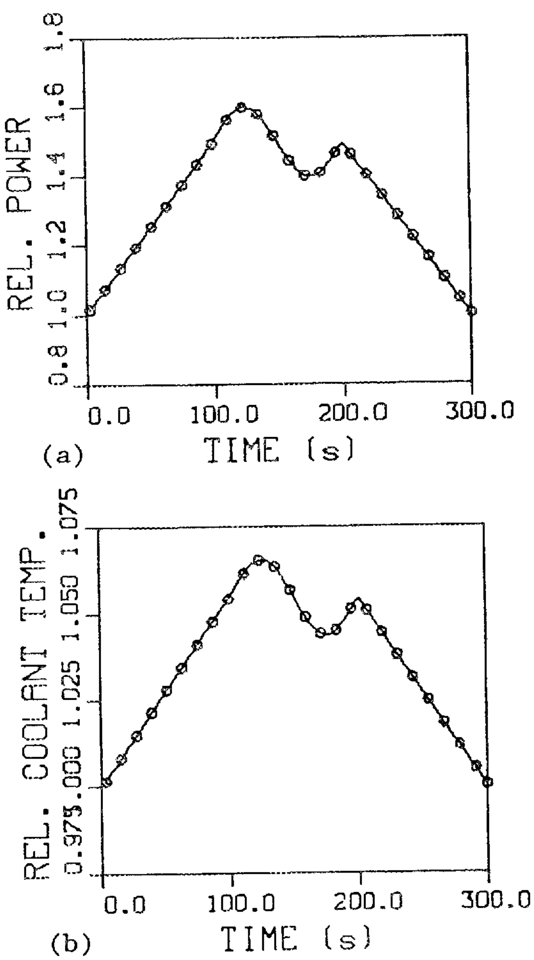

Fig. 3.3. Neutron density and outlet coolant temperature demand following. Solid lines represent the demand and circles the plant response: (a) relative neutron density and (b) relative outlet coolant temperature.

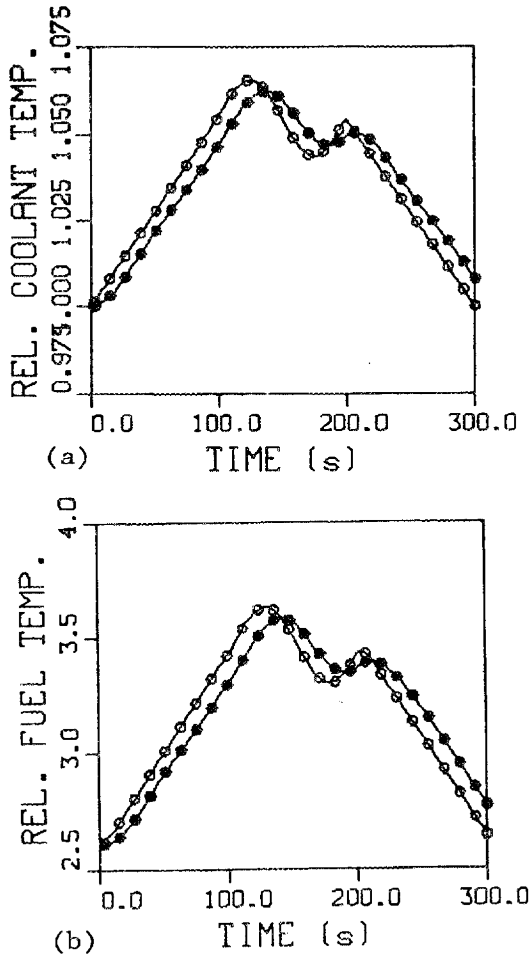

Fig. 3.4. Delay introduced by the detection process. Solid lines are the plant values, and black dots and circles represent the algorithm estimations for the measured and actual temperature respectively: (a) relative coolant temperature, and (b) relative fuel temperature.

4. OPTIMAL FILTERING, PARAMETER TRACKING, AND CONTROL OF NONLINEAR NUCLEAR REACTORS

The availability of fast and reliable microprocessors has opened the possibility of performing on-line numerical calculations to improve and optimize the way nuclear reactors are controlled. In particular, there is an increased interest[8] in improving the robustness of control algorithms when system behavior is affected by nonlinearities, unknown time-varying parameters, and noisy signals.

The following sections present a new microprocessor-based algorithm that is able to perform on-line filtering, parameter tracking, and control of a nonlinear nuclear reactor. A variational technique based on Pontryagin's Maximum Principle is used to estimate the system's state and parameters and to calculate the optimal control.

Three simultaneous optimizations are performed:

1. The estimate of the state variables is determined by the optimal matching of the noisy plant signals to the model.

2. The time-varying parameter is obtained by matching the filtered estimate to the control model.

3. The optimal controls are obtained by matching a set of prescribed demands.

To validate the algorithm, a nonlinear nuclear reactor was simulated in which the coolant feedback coefficient was an unknown time-varying parameter and the signals from the plant had additive noise. The plant was forced to follow demands in neutron density and outlet coolant temperature by adjusting two controls: (1) $u1$, reactivity, which was constrained to a given set of values; and (2) $u2$, inlet coolant temperature.

4.1 REFORMULATION OF THE OPTIMAL CONTROL PROBLEM

This section reviews the reformulation of the FTT optimal control problem.

Let

$$dy/dt = \mathbf{F}(\mathbf{y},\mathbf{u}) \tag{4-1}$$

represent the plant model, where $\mathbf{y}$ is the state variables and $\mathbf{u}$ the controls. Our goal is to find $\mathbf{u}(t)$ such that the system will follow a given set of demands, $\mathbf{d}$, in the sense that the cost function, defined as

$$J = \int_0^{tf} \{[\mathbf{d}-\mathbf{H}(\mathbf{y})]^T Q[\mathbf{d}-\mathbf{H}(\mathbf{y})] + \mathbf{u}^T R\mathbf{u}\} dt \quad , \tag{4-2}$$

is minimized. Q and R are weight matrices, which are allowed to change with time. Initial state $\mathbf{y}(o)$ and final state $\mathbf{Hy}(tf)$ are known, but tf is free.

It has been shown (see Sect. 3) that, if the system is in equilibrium at $t = o$ and $\mathbf{d}$ is a well-behaved function, the minimization problem is equivalent to the system:

$$d\mathbf{y}/dt = \mathbf{F}(\mathbf{y},\mathbf{u}) \quad , \tag{4-3}$$

$$d\mathbf{w}/dt = (d\mathbf{F}/d\mathbf{y})^T\mathbf{w} - (d\mathbf{H}/d\mathbf{y})Q(\mathbf{d}-\mathbf{H}(\mathbf{y})) \quad , \tag{4-4}$$

$$\mathbf{u} = R^{-1}\mathbf{w}^T(d\mathbf{F}/d\mathbf{u}) \quad , \tag{4-5}$$

$$\mathbf{y}(o)=\mathbf{yo} \ , \ \mathbf{w}(o)=\mathbf{o} \quad , \tag{4-6}$$

where $\mathbf{w}$ is the set of Lagrange multipliers or adjoints. The above reformulation of PMP can be achieved by integrating backwards the cost function, and the initial conditions are known only if the initial estate is in equilibrium. Under these special conditions, the calculation of the optimal control can be easily executed on-line in a microprocessor, because the classical TPBVP has been recast as an initial value problem.

4.2 STATE ESTIMATION: FILTERING

In this section the optimal control reformulation is applied to the problem of estimating the actual state of the plant from detector signals that are corrupted with additive noise.

Assuming that Eq. (4-1) represents a mathematical description of our system, define

$$\mathbf{s} = \mathbf{y}_d + \boldsymbol{\eta} \tag{4-7}$$

as the set of signals coming from the plant detectors, where $\mathbf{y}_d$ represents the detectors state variables and $\boldsymbol{\eta}$ represents an additive noise with zero mean.

Let us define $\mathbf{x}$ as the estimated plant state. The dynamic estimation of $\mathbf{x}$ can be obtained from

$$d\mathbf{x}/dt = \mathbf{G}(\mathbf{x},\mathbf{u}) + \mathbf{v} \quad , \tag{4-8}$$

where $\mathbf{G}$ is an approximated model of the plant (predictor) and $\mathbf{v}$ is the dynamic correction (corrector) that can be obtained from the minimization of the cost function,

$$J_F = \int_0^{tf} \{[\mathbf{s}-\mathbf{x}_d]^T Q_f [\mathbf{s}-\mathbf{x}_d] + \mathbf{v}^T R_f \mathbf{v}\} dt \quad . \tag{4-9}$$

4.3 PARAMETER TRACKING

This section shows how the reformulation of the optimal control problem can be used to update the plant time-varying parameters.

Assume that there is a set of parameters, $\mathbf{a}$, which can change arbitrarily with time. Our control model needs to be updated on-line, otherwise, we cannot guarantee that the calculated control will be optimal. The updating of the control model can be achieved by applying the reformulation of the optimal control problem presented in Sect. 4.2. In this case we assume that the magnitude of $\mathbf{a}$ will be such as to minimize the cost function,

$$J_P = \int_0^{tf} \{[\mathbf{x}-\mathbf{m}]^T Q_p [\mathbf{x}-\mathbf{m}] + \mathbf{a}^T R_p \mathbf{a}\} dt \quad , \tag{4-10}$$

where $\mathbf{m}$ represents the control model state variables.

4.4 OPTIMAL CONTROL

At this point, our algorithm is able to estimate the actual state variables and the time-varying parameter magnitude; therefore, we have an adaptive model to which again we can apply the reformulated optimal control problem to obtain the controls necessary to follow the demands. Now we have to minimize the cost function, defined as

$$J_C = \int_0^{tf} \{[\mathbf{d}-\mathbf{H}\mathbf{m}]^T Q_c [\mathbf{d}-\mathbf{H}\mathbf{m}] + \mathbf{u}^T R_c \mathbf{u}\} dt \quad . \tag{4-11}$$

4.5 THE ALGORITHM

As stated before, our goal is to develop an algorithm that is able to update the control model by estimating the state variables and time-varying parameters while calculating the optimal control. This objective is achieved by minimizing the three cost functions, J_F [Eq. (4-9)], J_P [Eq. (4-10)], and J_C [Eq. (4-11)], independently and simultaneously. The set of equations to solve can be summarized as follows:

$$d\mathbf{x}/dt = \mathbf{G}(\mathbf{x},\mathbf{a},\mathbf{u}) + \mathbf{v} \quad , \tag{4-12}$$

$$d\mathbf{m}/dt = \mathbf{G}(\mathbf{m},\mathbf{a},\mathbf{u}) \quad , \tag{4-13}$$

$$d\mathbf{w}_f/dt = (d\mathbf{G}/d\mathbf{x})^T \mathbf{w}_f - Q_f(\mathbf{s}-\mathbf{x}_d) \quad , \tag{4-14}$$

$$d\mathbf{w}_p/dt = (dG/d\mathbf{m})^T\mathbf{w}_p - Q_p(\mathbf{x}-\mathbf{m}) \quad , \tag{4-15}$$

$$d\mathbf{w}_c/dt = (dG/d\mathbf{x})^T\mathbf{w}_c - (d\mathbf{H}(\mathbf{m})/d\mathbf{m})Q_c(\mathbf{d}-\mathbf{H}(\mathbf{m})) \quad , \tag{4-16}$$

$$\mathbf{v} = (R_f)^{-1}\mathbf{w}_f{}^T(dG/d\mathbf{v}) \quad , \tag{4-17}$$

$$\mathbf{a} = (R_p)^{-1}\mathbf{w}_p{}^T(dG/d\mathbf{a}) \quad , \tag{4-18}$$

$$\mathbf{u} = (R_c)^{-1}\mathbf{w}_c{}^T(dG/d\mathbf{v}) \quad , \tag{4-19}$$

$$\mathbf{m}(o) = \mathbf{x}(o) = \mathbf{y}(o) = \mathbf{y}_o \quad , \tag{4-20}$$

$$\mathbf{w}_f(o) = \mathbf{w}_p(o) = \mathbf{w}_c(o) = \mathbf{o} \quad . \tag{4-21}$$

Equations (4-12) to (4-16) can be solved simultaneously with the initial conditions given by Eqs. (4-20) and (4-21) by using any standard differential equation solver. Equations (4-17) to (4-19) return the filter corrector, **v**, the unknown parameters, **a**, and the optimal controls, **u**.

4.6 APPLICATION TO A NONLINEAR NUCLEAR REACTOR

The algorithm presented in this section has been applied to a nonlinear reactor model. The plant was simulated with a four-dimensional model and three detectors. During the transient, the feedback coefficient due to the coolant temperature was changing sinusoidally with time. The signals coming from the simulated plant were corrupted with additive noise. The plant was forced to follow demands in neutron density and outlet coolant temperature by adjusting two control inputs: (1) reactivity, which was constrained to a given value, and (2) inlet coolant temperature.

Figure 4.1 shows how both demands in power and outlet coolant temperature were followed by the plant despite the parameter changes and constraints in the controls. Figure 4.2 shows how the algorithm was able to update the coolant temperature feedback parameter during the transient. Figure 4.3 shows the controls that were necessary to follow the transient. Finally, Fig. 4.4 shows how the variational filter eliminates the additive noise from the plant signals.

4.7 CONCLUSIONS

An optimal filtering, parameter tracking, and control algorithm has been developed that allows one to find on-line solutions for demand-following problems in the cases in which noisy signals, nonlinearities, and time-varying parameters invalidate other known algorithms. An important result has been the recasting of Pontryagin's Maximum Principle technique for nonlinear systems as the solution to differential equations with initial conditions. The algorithm has been applied successfully to a nonlinear nuclear reactor model. Using plant sensor signals, all the state variables were estimated, and the time-varying

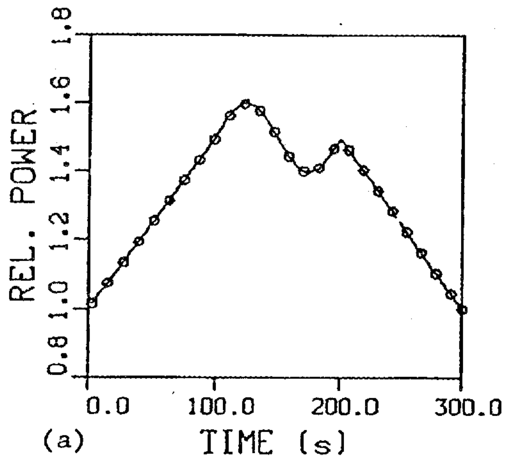

(a)

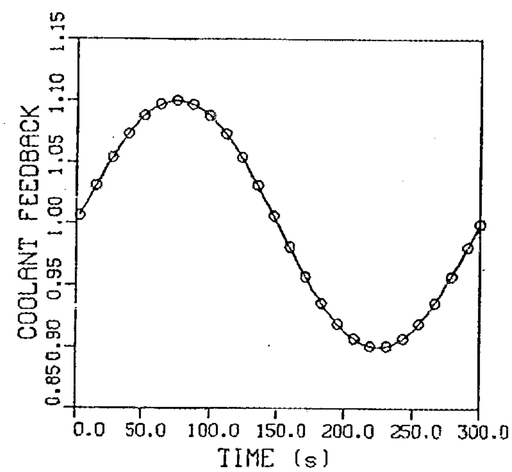

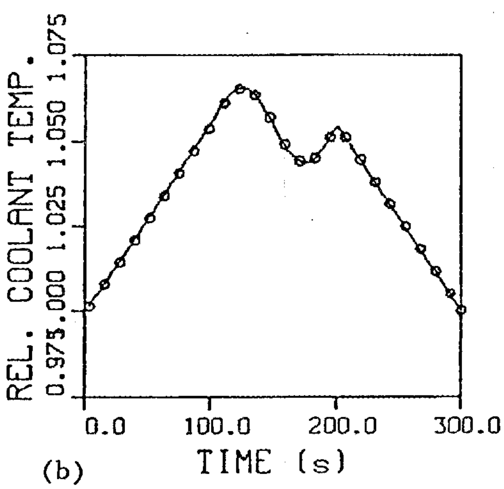

(b)

Fig. 4.1. Power and outlet coolant temperature demand following. (a) Demand on power (solid line) and plant power (circles) vs time, and (b) demand on hot leg temperature (solid line) and plant hot leg temperature (circles) vs time.

Fig. 4.2. Time-varying parameter update. Plant coolant feedback coefficient (solid line) and algorithm estimate (circles) vs time.

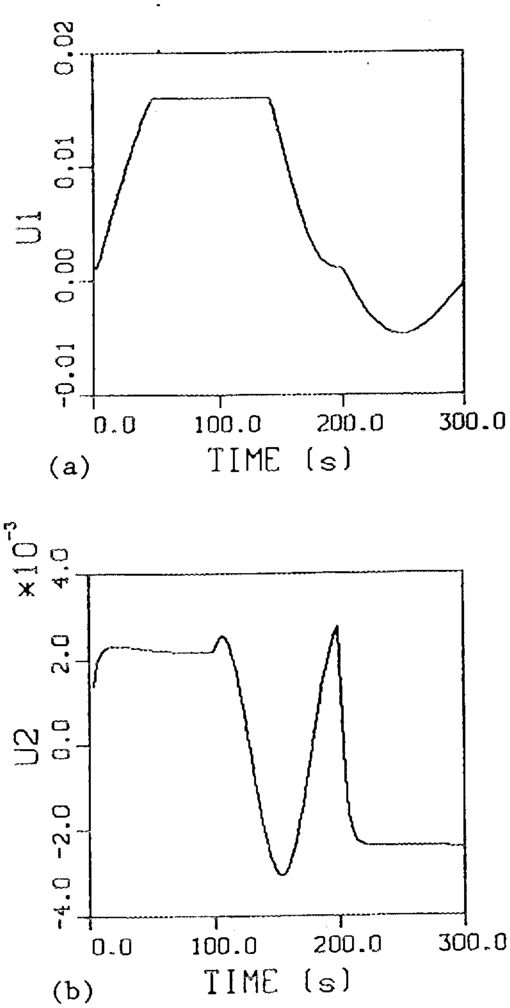

Fig. 4.3. Optimal controls: (a) *u*1, reactivity, which was constrained to be less than 0.016, and (b) *u*2, inlet coolant temperature change.

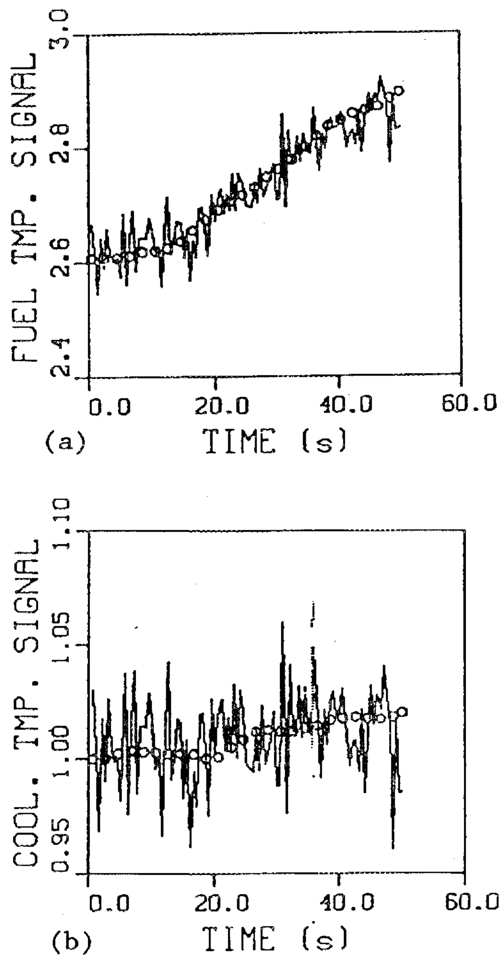

Fig. 4.4. Optimal filtering: (a) coolant temperature detector signal (solid line) and algorithm filtered estimates (circles) vs time, and (b) fuel temperature detector signal (solid line) and algorithm filtered estimates (circles) vs time.

parameter was updated during the transient, allowing an adaptive optimal control calculation. We can conclude that this new formulation of the optimal control problem provides a suitable methodology for on-line, microprocessor-based applications.

5. REACTOR MONITORING APPLICATIONS

5.1 TRANSIENT REACTIVITY MONITOR

This section presents a technique to estimate excess reactivity values during transient conditions, which can be used to determine time-dependent reactivity coefficients. The present technique is based on optimal control theory. A control strategy is set up to minimize the difference between the measured neutron flux and a mathematical model of the reactor dynamics. The control variable is the parameter to be determined which, in this case, corresponds to the excess reactivity. The optimal control equations have been solved and applied to several example cases. Excellent agreement is obtained between estimated and actual transient reactivity values.

5.1.1 Background

Reactivity feedback coefficients are customarily evaluated using detailed neutronic codes, and the calculated values are verified *a posteriori* against results of steady state experiments.[9] In those experiments, the neutron flux is increased, then the reactor is allowed to stabilize, and the excess reactivity is estimated from the new control rod position. In general, though, reactivity coefficients are time-dependent because of fuel expansion effects that produce geometry changes. In those cases, the steady state coefficients might not represent accurately the prompt coefficients; indeed, they might even have different signs.

5.1.2 Theory

The approach taken in this implementation is to apply an optimal control technique to determine excess reactivity values during transients. To this end, a control strategy is set up to minimize the difference between the measured neutron flux and a mathematical model of the reactor dynamics. The control variable is the parameter to be determined that, in this case, corresponds to p, the excess reactivity. Mathematically, we attempt to minimize the following functional:

$$J = \int_0^{tf} [(n_m - n)^2 Q + p^2] dt \quad , \tag{5-1}$$

where Q is an adjustable weighing factor, n_m is the measured neutron flux, and n is the neutron flux predicted by a reactor dynamic model, expressed as

$$d\mathbf{x}/dt = \mathbf{F}(\mathbf{x},\mathbf{p}) \quad , \tag{5-2}$$

where x is the vector of state variables, including n, and $\mathbf{F}$ is a vector function describing the reactor dynamics.

The optimal value of p that minimizes the above cost function can be readily obtained by the introduction of state variable adjoints, w, that are given by the following relations:

$$d\mathbf{w}/dt = (d\mathbf{F}/d\mathbf{x})^{T}\mathbf{w} - Q(n_{m}-n) \quad , \tag{5-3}$$

$$p = -\mathbf{w}(d\mathbf{F}/dp) \quad , \tag{5-4}$$

with boundary conditions

$$n(0) = n_{m}(0) \quad , \tag{5-5}$$

$$\mathbf{w}(0) = 0 \quad . \tag{5-6}$$

5.1.3 Application

To illustrate this technique, we have applied it to a dynamic model of the ANS reactor.[10] This model includes a point kinetics representation of the neutron field with thermohydraulic feedback that is composed of fuel, core coolant, the in-vessel bypass region, and the reflector region.

Using the above model as a reference reactor, transients have been performed by moving control rods under several reactivity coefficients assumptions. These transients have been analyzed using the technique outlined in the previous equations to obtain the transient reactivity. To this end, a reduced model was used that consisted only of a one-delayed-group point kinetics model, without any explicit representation of the feedback terms.

That is, the reference model used to estimate the transient reactivity can be expressed as

$$d\mathbf{x}/dt = \mathbf{F}(\mathbf{x},p) \quad , \tag{5-7}$$

$$\mathbf{x}^{T} = (n,c) \quad , \tag{5-8}$$

where n is the neutron flux, c is the delayed neutron precursor concentration, and $\mathbf{F}(\mathbf{x},p)$ is the standard point kinetics representation with a single group of delayed neutrons.

5.1.4 Results

Figure 5.1 presents a typical result of these analyses. This figure shows the transient reactivity estimated from the present technique along with the reactivity from the reference model. Superimposed on the same figure are the estimated feedback reactivity and the actual control rod reactivity used for the transient. This particular transient (a sinusoidal, followed by a constant, followed by a ramp in reactivity) highlights the fact that the present technique is able to extract the transient reactivity from the measured neutron flux, even under extreme and unusual conditions.

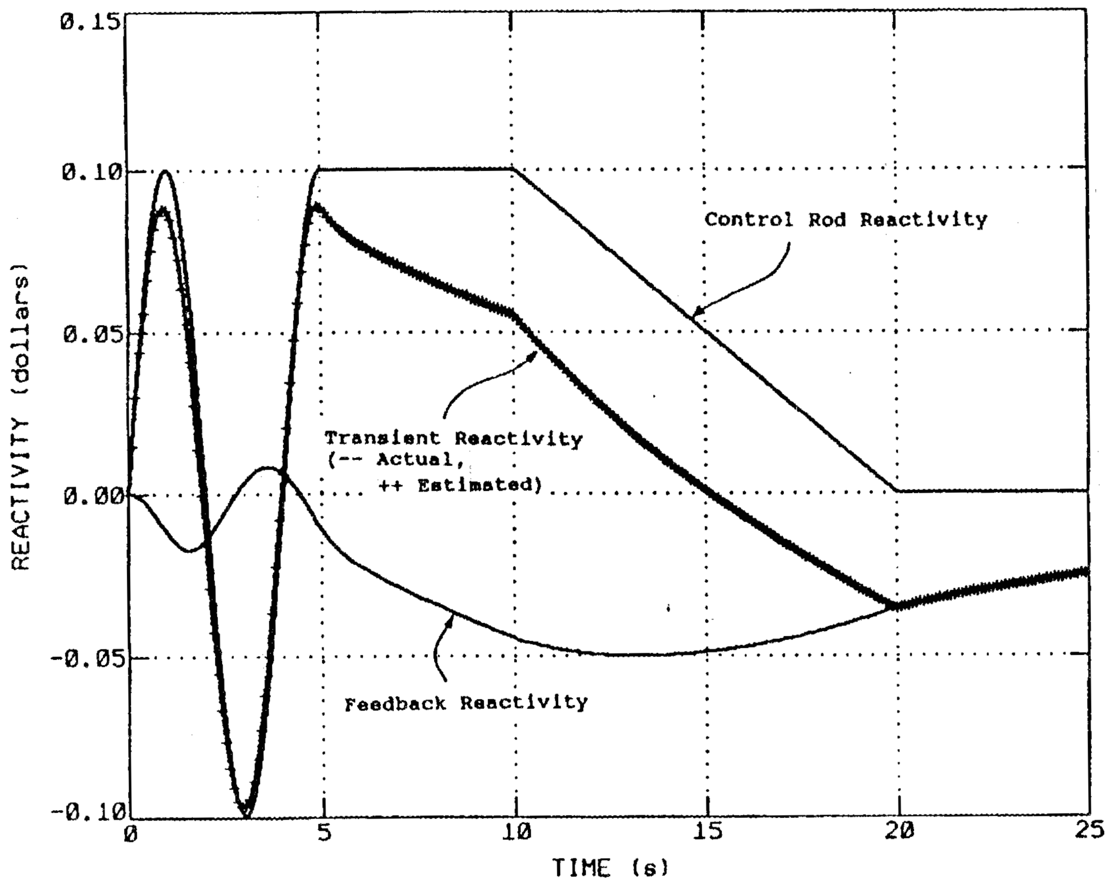

Fig. 5.1. The estimated transient reactivity (crosses) shows excellent agreement with the actual transient reactivity (solid line).

5.2 STATE ESTIMATOR FOR PWR

This section documents an algorithm designed to estimate the state variables of nonlinear dynamical systems. The present algorithm relies on measurements of detector signals that are in general corrupted by additive noise, and it attempts to estimate the actual value of the state variables based on a model representation.

5.2.1 Background

Optimal control algorithms require the knowledge of many of the system state variables. In practical cases, only a subset of these variables is measured, and values of this subset are not well known because of noise contamination. A common technique used for estimating unmeasured state variables is known as Kalman filtering that is based on linearized models and, thus, it may fail under special conditions when nonlinearities are dominant.

5.2.2 Theory

The goal of the present algorithm is to update an estimate, y, of the vector of state variables, $\mathbf{x}$, when only a subset of signals, s, from the plant is measured. In addition, the measured signals are allowed to be contaminated by noise. The detection process can be described mathematically as $\mathbf{s} = \mathbf{G}(\mathbf{x}) + \boldsymbol{\eta}$, where $\boldsymbol{\eta}$ is a vector of additive noises and $\mathbf{G}(\mathbf{x})$ is a general vector function relating the measured signals with the actual plant variables. The state estimates are assumed to satisfy the following relation,

$$dy/dt = \mathbf{f}(\mathbf{y}) + \mathbf{e} \quad , \tag{5-9}$$

where $\mathbf{f}(\mathbf{y})$ is an approximate plant model that acts as a predictor of the next estimate and $\mathbf{e}$ acts as the corrector. The present algorithm calculates $\mathbf{e}$ based on the PMP by minimizing the cost function,

$$J = \int_0^{tf} [(\mathbf{s}-\mathbf{G}(\mathbf{x}))^T Q(\mathbf{s}-\mathbf{G}(\mathbf{x})) + \mathbf{e}^T R\mathbf{e}]\ dt \quad , \tag{5-10}$$

where Q and R are weight matrices.

Following the dual adjoint technique (see Sect. 2), this minimization results in the following equations for the adjoints $\mathbf{w}$ and $\mathbf{e}$:

$$\mathbf{w} = (d\mathbf{f}/d\mathbf{y})^T\mathbf{w} \quad - \quad Q(\mathbf{s}-\mathbf{G}(\mathbf{y}))\ (d\mathbf{G}/d\mathbf{y}) \quad , \tag{5-10}$$

$$\mathbf{e} = -R^{-1}\mathbf{w} \quad , \tag{5-11}$$

5.2.3 Validation

An example of application of the present technique has been produced using a nonlinear model of a PWR, which includes a point kinetics representation of the neutron field, a single-node representation of the fuel and coolant dynamics, and reactivity feedback. The detection process is modeled, including detector time delays. A transient was induced in the plant model by ramping the inlet coolant temperature, and detection noise was added to the measured signals (power and fuel and coolant temperatures). Figure 5.2 shows the results of the filtering algorithm, which is a comparison between the detector responses with and without noise (solid lines) and the signal estimated by the present algorithm (dots). Satisfactory agreement is found between the estimated and actual transients despite the presence of a significant amount of measurement noise. Figure 5.3 shows how the present algorithm is able to update the unmeasured state variables.

5.2.4 Summary

A successful algorithm has been proposed for the estimation of unmeasured state variables based on the values of some observed variables that are contaminated by noise and detector time delays.

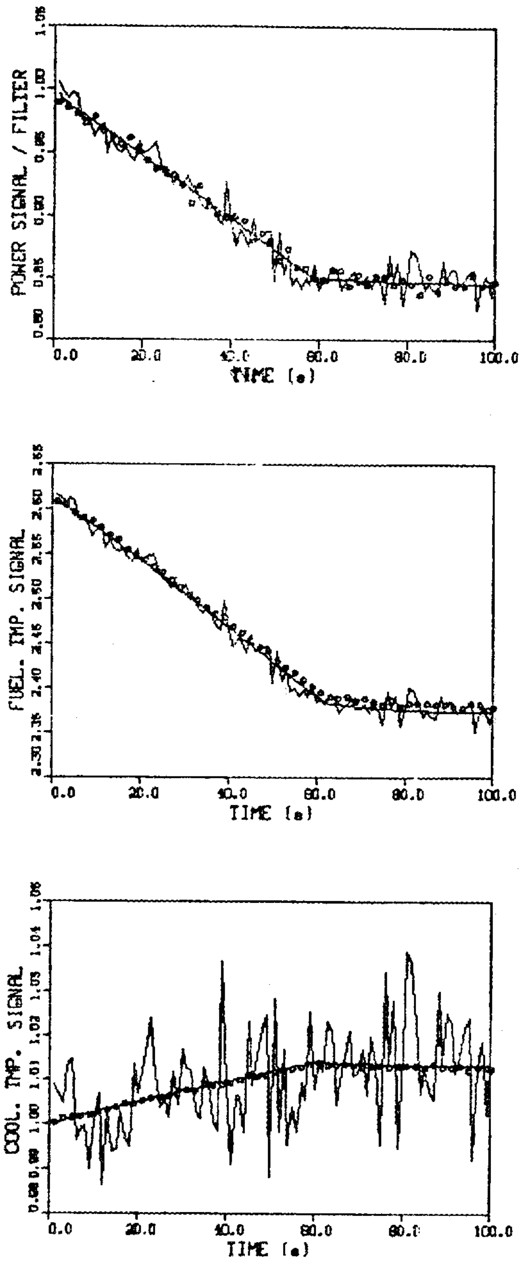

Fig. 5.2. Comparison of the detector responses with and without noise (solid lines) with the signal estimated by the present algorithm (dots).

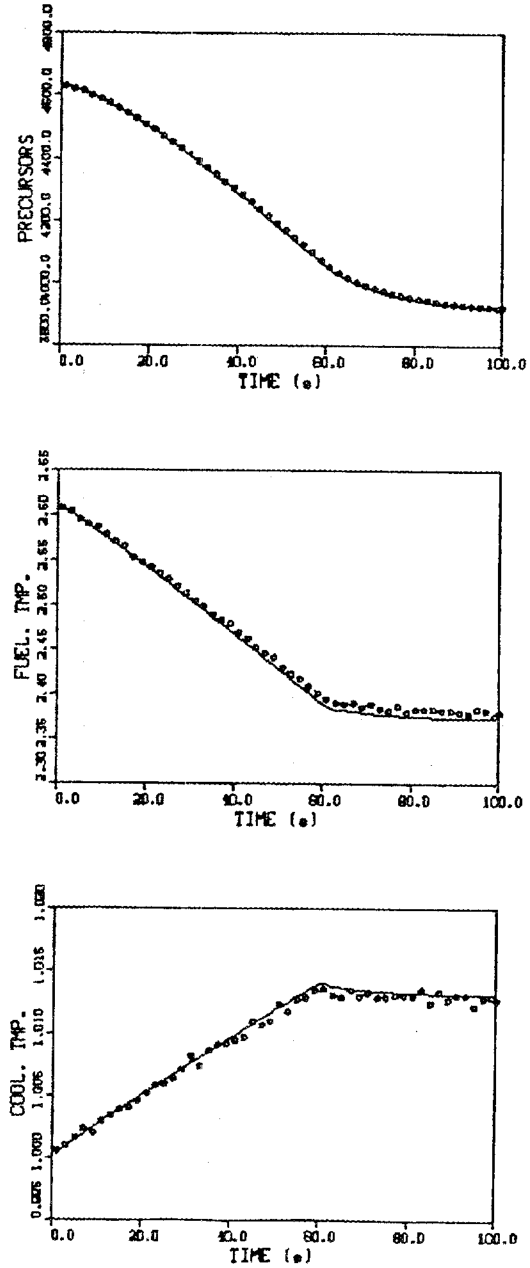

Fig. 5.3. Comparison of the unmeasured state variables estimated by the algorithm (dots) and their actual plant value (solid line).

6. A COMPARISON BETWEEN OPTIMAL CONTROL AND PI CONTROL: BWR POWER CONTROL DESIGN

6.1 THE BWR MODEL

The dynamic behavior of a BWR can be represented by the following model:

$$dP/dt = P(\rho+\alpha T-\beta)/\Lambda + \lambda C \quad ; \tag{6-1}$$

$$dC/dt = \beta P/\Lambda - \lambda C \quad ; \tag{6-2}$$

$$dT/dt = a_1(P-P_o) - a_2 T \quad ; \tag{6-3}$$

$$d^2\rho/dt^2 + (6/\tau)d\rho/dt + (12/\tau)\rho = (K/\tau^2)(P/U)T \quad ; \tag{6-4}$$

$$P_o = 0.6 + (0.4/0.6)(U-0.4) \quad ; \tag{6-5}$$

$$\tau = 0.65/U \quad ; \tag{6-7}$$

where P represents the reactor power, C the delayed neutron precursor concentration, T the fuel temperature, and ρ the void fraction feedback. The core flow is represented by U (control). It has been shown[11] that this simplified model is able to emulate fairly accurately the nonlinear behavior of a BWR.

6.2 PI CONTROL DESIGN

The PI control is designed in the standard fashion,

$$U = U_p + U_i \quad , \tag{6-8}$$

where U_p is the proportional part given by

$$U_p = (D-P)q \quad , \tag{6-9}$$

and U_i is the integral part given by

$$dU_i/dt = (D-P)k \quad , \tag{6-10}$$

where D represents the demand and q and k are the gain constants. The weights q and k are calculated such that they guarantee the stability of the system; that is, all the real parts of the system's eigenvalues are negative. Unfortunately, it is necessary to linearize the model to perform the stability analysis, and the optimal gains are not always obvious.

Figure 6.1 presents the reactor response to a ramp demand in power from 100% to 60% (that should correspond to a change in flow from 100% to 40%) when the reactor is controlled using a PI technique. In this case, the linearization necessary for the PI design was performed at 100% power. The values for the gains that make the system stable at this

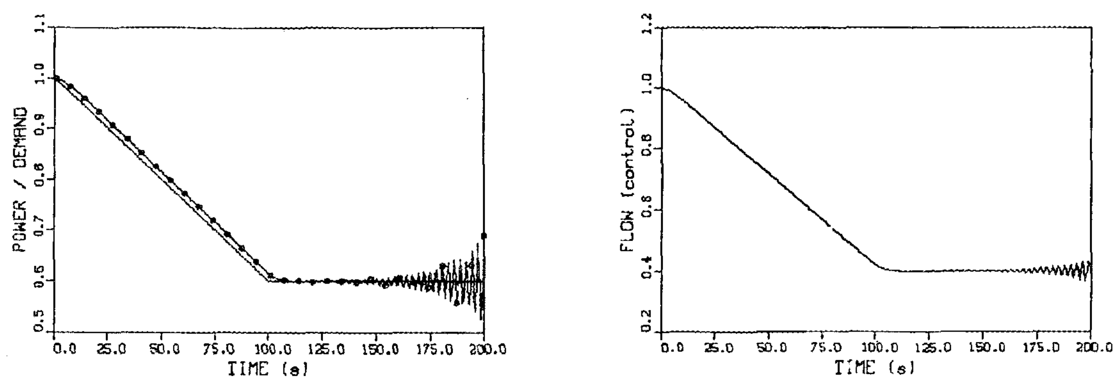

(a) (b)

Fig. 6.1. Reactor response to a power ramp demand from 100% to 60%, with power controlled by a PI technique. Flow is the controlled variable: (a) power and (b) required flow control.

power were calculated. As Fig. 6.1 shows, these gains are able to stabilize the system at 100% power and to make the power follow the imposed demand, but we can see that at the end of the transient the system becomes unstable. One of the system's eigenvalues has become positive. A divergent oscillatory behavior can be seen from the figure.

6.3 OPTIMAL CONTROL DESIGN

In our design we are going to assume that a part of the BWR model is known. In particular, we assume that we have a dynamic model for the power, precursors, and temperature of the fuel. The void fraction feedback dynamic is unknown to the control system designer. We also assume that a plant power signal is available.

The knowledge of the state variables is fundamental to design and optimal control; therefore, our first goal is to obtain the unknown variables, the void fraction feedback, and fuel temperature. This goal can be achieved by applying optimal control theory (see Sect. 2) to the so-called state estimation problem. The idea is to find the optimal value of ρ that minimizes, in the least-squares sense, the error between the measured power signal and our control model.

Once we have obtained the unknown variable, the optimal control can be calculated following the same technique: We want to obtain the best U that minimizes the error between the demand and the control model.

To improve the stability of the control algorithm, we have also included in the minimization the error between the derivative of the demand and the derivative of the state variables.

Figure 6.2 resumes the computer simulation results: (a) shows how the control algorithm is able to follow the demand and to stabilize the system at any power, (b) shows how the algorithm is able to track the unknown variable (void fraction feedback), and (c) shows the control action given by the algorithm.

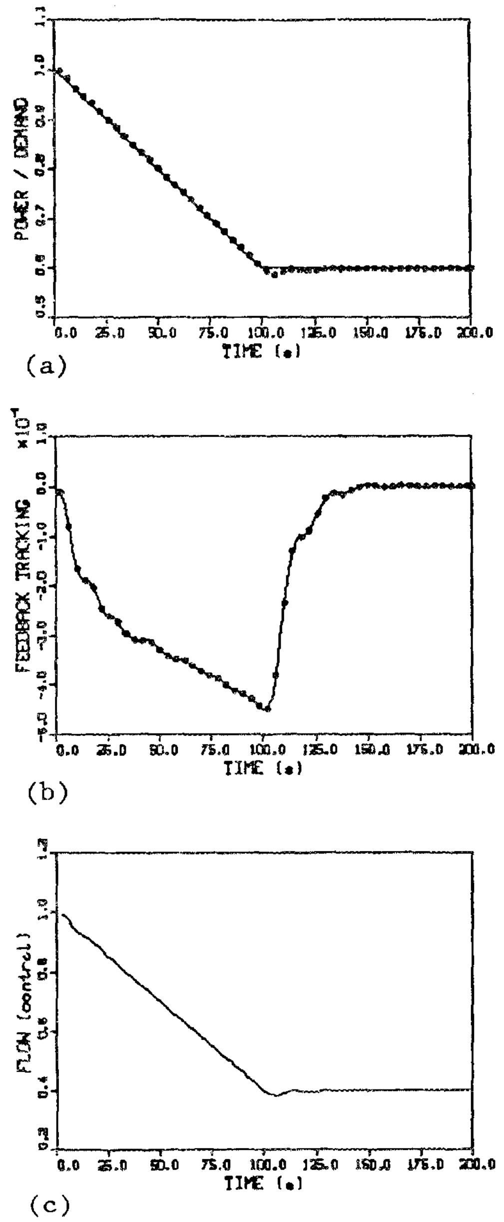

Fig. 6.2. Reactor response to a power ramp demand from 100% to 60%. Power is controlled by the optimal control technique, with the flow being the controlled variable: (a) power, (b) void reactivity feedback, actual (solid line) and estimated (circles), and (c) the required flow control.

7. OPTIMAL CONTROL OF UNCERTAIN NONLINEAR SYSTEMS: AN APPLICATION TO A TWO-LINK ROBOTIC ARM

The availability of fast and reliable microprocessors has opened the possibility of performing on-line numerical calculations to improve and optimize the manner in which mechanical manipulators are controlled. In particular, there is a general interest (see ref. 8) in increasing the robustness of control algorithms when system behavior is affected by nonlinearities, or when a relevant part of the system dynamic is unknown a priori for the control designer.

This section presents a new microprocessor-based algorithm that is able to perform uncertainty-tracking and control the mechanical manipulator. A variational technique based on Pontryagin's Maximum Principle is used to update and decompose the control model and to calculate the optimal control.

Three simultaneous optimizations are performed: (1) The trajectory in generalized coordinates is obtained by matching the kinematic model of the arm to the prescribed trajectory in Cartesian coordinates. (2) The model's unknown terms are obtained by matching the signals from the arm's detectors to the control model. (3) The optimal controls are obtained by matching the trajectory in generalized coordinates to the updated dynamic model.

To validate the algorithm, a system representing a two-link robotic arm was simulated. In the control model the coupling and friction terms were unknown. The robot was forced to follow a prescribed trajectory and to pick up an unknown mass.

7.1 THE DUAL ADJOINT TECHNIQUE

This section reviews the reformulation of the FTT optimal control problem presented in Sect. 2.

Let

$$dy/dt = \mathbf{F}(\mathbf{y},\mathbf{u}) \qquad (7\text{-}1)$$

represent the plant model, where $\mathbf{y}$ is the state variables and $\mathbf{u}$ the controls. Our goal is to find $\mathbf{u}(t)$ such that the system will follow a given set of demands, $\mathbf{d}$, in the sense that the cost function defined as

$$J = \int_0^{tf} \{[\mathbf{d}-\mathbf{H}(\mathbf{y})]^T Q[\mathbf{d}-\mathbf{H}(\mathbf{y})] + \mathbf{u}^T R\mathbf{u}\}dt \qquad (7\text{-}2)$$

is minimized. Q and R are weight matrices, which are allowed to change with time. The initial state $\mathbf{y}(o)$ and final state $\mathrm{H}(\mathbf{y}(tf))$ are known, but tf is free.

If the system is in equilibrium at $t = 0$ and **d** is a well behaved function, the minimization problem is equivalent to the solution of the following set of equations:

$$dy/dt = \mathbf{F}(\mathbf{y},\mathbf{u}) \quad , \tag{7-3}$$

$$d\mathbf{w}/dt = (d\mathbf{F}/d\mathbf{y})^T\mathbf{w} - (d\mathbf{H}/d\mathbf{y})Q(\mathbf{d}-\mathbf{H}(\mathbf{y})) \quad , \tag{7-4}$$

$$\mathbf{u} = R^{-1}\mathbf{w}^T(d\mathbf{F}/d\mathbf{u}) \quad , \tag{7-5}$$

$$\mathbf{y}(o) = yo \ ; \ \mathbf{w}(o) = o \quad , \tag{7-6}$$

where **w** is the set of Lagrange multipliers or adjoints. The above reformulation of PMP can be achieved by integrating backwards the cost function, and the initial conditions are known only if the initial estate is in equilibrium. Under this special condition the calculation of the optimal control can be easily executed on-line, in a microprocessor, because the classical TPBVP is recast into an initial value problem.

7.2 TRAJECTORY PRESCRIPTION

This section shows how the arm angular velocities, **d**, which locate the end-effector on the trajectory, can be obtained by applying the reformulated optimal control problem.

Let **tra**(e) be a parametric representation of the trajectory in Cartesian coordinates. First we map the real time t into the parameter e by applying

$$e = 1/2[1-cos(\pi t/t_f)] \quad . \tag{7-7}$$

By the choice of this mapping we obtain directly the steady state initial and final conditions. Now we can calculate the angular velocities by minimizing the cost function,

$$J_T = \int_0^{tf} ([\mathbf{tra}-G(\mathbf{d})]^T Q[\mathbf{tra}-G(\mathbf{d})] + \mathbf{d}^T R\mathbf{d})dt \quad , \tag{7-8}$$

where G(**d**) represents the transformation from generalized, **d**, to Cartesian coordinates.

7.3 UNCERTAINTY TRACKING

This section shows how the reformulation of the optimal control problem can be used to update the system's unknown terms.

Assume that there is a set of unknown terms, **a**, which can change arbitrarily with time. Our control model needs to be updated on-line, otherwise we cannot guarantee that the calculated control will be optimal. The updating of the control model can be achieved by applying the reformulation of the optimal control problem. In this case, we assume that the magnitude of the unknown terms, **a**, will be such that the cost function,

$$J_P = \int_0^{tf} \{[\mathbf{x}-\mathbf{m}]^T Q_p [\mathbf{x}-\mathbf{m}] + \mathbf{a}^T R_p \mathbf{a}\} dt \quad , \tag{7-9}$$

is a minimum, where **m** represents the control model state variables and **x** the detector signals.

7.4 SYSTEM DECOUPLING AND DECOMPOSITION

Often the plant's dynamic model involves a large number of differential equations. In this case, it may be convenient to decompose the large model into a set of decoupled subsystems. The uncertainty tracking method can be used to achieve an efficient decomposition without losing too much information.

Let us assume that

$$d\mathbf{x}/dt = \mathbf{F}(\mathbf{x},\mathbf{u}) \tag{7-10}$$

represents the mathematical model of the plant that we wish to control, where the vector **x** represents the n state variables and **u** represents the m controls. Let

$$d\mathbf{x}_i/dt = \mathbf{F}_i(\mathbf{x}_i,\mathbf{u}_i) + \mathbf{p}_i \quad , \qquad i = 1,\ k \tag{7-11}$$

represent a set of k subsystems formulated in such a way that they are uncoupled. To guarantee that this set of subsystems represents the whole system, we introduce the unknown set of functions, $\mathbf{p}_i$, whose values at time t can be obtained by the optimal matching of the signals coming from the detectors, with the values for the state variables given by the numerical integration of the subsystem's mathematical models. Actually, this problem can be formulated as an optimal control problem. We want to know which are the values of controls (unknown function p) that make the subsystems follow the demand (detector signals).

7.5 OPTIMAL CONTROL

At this point, our algorithm is able to update the control model; therefore, we have an adaptive model to which we can apply the reformulated optimal control problem to obtain the controls necessary to follow the demands. Now, to implement the demand-following capabilities, we have to minimize the cost function, defined as

$$J_C = \int_0^{tf} \{[\mathbf{d}-\mathbf{m}]^T Q_c [\mathbf{d}-\mathbf{m}] + \mathbf{u}^T R_c \mathbf{u}\} dt \quad . \tag{7-12}$$

7.6 APPLICATION TO A ROBOTIC ARM

To validate the algorithm, a computer simulation of a two-link robotic arm was developed which included the friction terms. The control problem is to determine the set of torques to be supplied to the arm so that its end-effector moves along a prescribed trajectory (the trajectory is given in Cartesian coordinates). In the control model, the coupling and friction terms are considered unknown; therefore, it is necessary to update their values during the transient. Moreover, the arm must pick up an object whose weight is changing with time.

Figure 7.1 shows the motion of the robotic arm along the trajectory. The arm's tasks are to follow the given trajectory (discrete line marked with the symbol +) and to pick up the unknown time-varying mass (graphically represented by a black disk).

7.7 CONCLUSIONS

This section presents a novel algorithm for the control of mechanical manipulators based on optimal control theory.

This new algorithm provides a suitable methodology for control problems in which only a part of the dynamic model of the robot is available to the designer. We have shown that this method can be applied to (1) transform coordinates, (2) update and decouple the control model, and (3) obtain the control inputs. The algorithm has been validated with a computer simulation of a two-link robotic arm.

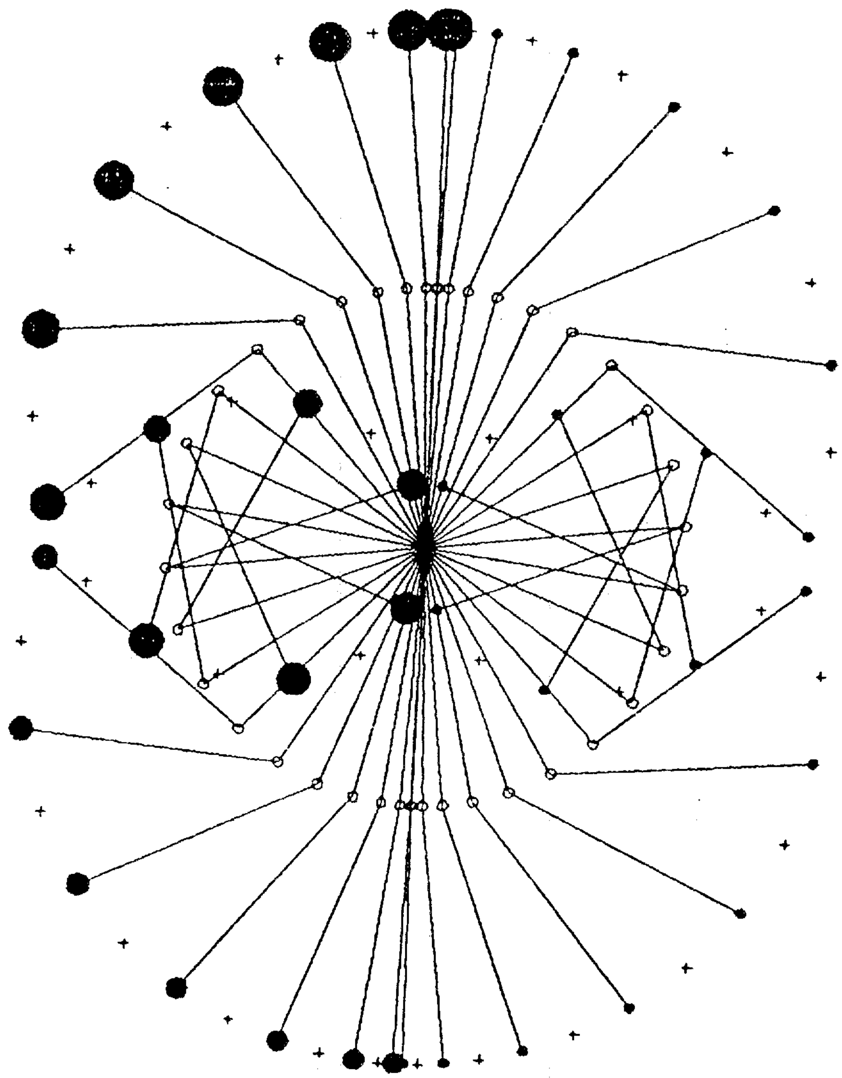

Fig. 7.1. Motion of the robotic arm along the trajectory. The arm task is to follow the given trajectory (discrete line marked with the symbol +) and to pick up the unknown time-varying mass (graphically represented by a black disk).

8. THE HAMILTON-JACOBI APPROACH

We have seen in previous sections how easy it is to implement the so-called dual adjoint technique. Unfortunately, this is not an optimal solution to the problem, and, as shown in Sect. 2, it will not work for unstable systems in general. In this section the more powerful Hamilton-Jacobi approach is used. To illustrate the technique, a mechanical manipulator control is designed.

8.1 THE HAMILTON-JACOBI EQUATION

This section reviews the formulation of the Hamilton-Jacobi approach to optimal control presented in Sect. 2.

Let us study the dynamic behavior of the cost function. First we define a dynamic cost function as

$$J(t) = \int_0^t V(x,u)\ d\tau \quad . \tag{8-1}$$

Taking the total derivative of $J(t)$ with respect to t,

$$J_t = -[J_x dx/dt - V(x,u)] \quad , \tag{8-2}$$

and defining the Hamiltonian as

$$H(J_x,x,u) = J_x dx/dt - V(x,u) \quad , \tag{8-3}$$

we obtain

$$J_t = -H(J_x,x,u) \quad . \tag{8-4}$$

Equation (8-4) is known as the Hamilton-Jacobi equation in classical mechanics. To minimize the temporal evolution of $J(t)$, we need to select u (the control) such that it minimizes the Hamiltonian. Also, we need to keep the value of the Hamiltonian constant and equal to zero during the evolution of the system.

The solution of the Hamilton-Jacobi equation can be really difficult, especially for multidimensional nonlinear systems. As shown in Sect. 2, some simplification can be obtained by transforming the cost function.

8.2 APPLICATION TO A MECHANICAL MANIPULATOR

This section presents in detail the design process of a closed-loop control algorithm for a mechanical manipulator. First, a model of the mechanical arm is developed using the Lagrange theory. Second, the control algorithm is designed using the Hamilton-Jacobi approach. Two different formulations for the cost function are solved and compared.

Because of the simplicity of this model, all calculations are made analytically.

8.2.1 The Model

The most powerful way of developing a dynamic model for a mechanical manipulator is to obtain the Lagrange-Euler equations in generalized coordinates.

Let us consider a one-link manipulator. For simplicity, we have assumed that all mass, m, is concentrated in the end-effector. The easiest approach to writing the Lagrangian in generalized coordinates (in this case polar coordinates) is to write it first in Cartesian form and then transform it to polar. In our case, the Lagrangian is

$$L = 1/2\ m(v^2_x+v^2_y) - mgy \quad . \tag{8-5}$$

The coordinates transformation is given by

$$x = r\sin(\theta) \quad , \tag{8-6}$$

$$y = -r\cos(\theta) \quad ; \tag{8-7}$$

therefore,

$$v_x = -r\cos(\theta) d\theta/dt \quad , \tag{8-8}$$

$$v_y = r\sin(\theta) d\theta/dt \quad , \tag{8-9}$$

After elementary algebraic manipulation, we can obtain the Lagrangian in polar coordinates as

$$L = 1/2m(r d\theta/dt)^2 + mgr\cos(\theta) \quad . \tag{8-10}$$

The Lagrange equation is formulated as

$$T = d/dt(L_{[d\theta/dt]}) - L_\theta \quad , \tag{8-11}$$

where T represents the torque. Introducing Eq. (8-10) into Eq. (8-11) leads to the dynamic equation for the mechanical manipulator:

$$d^2\theta/dt^2 = -(g/r)\sin(\theta) + T/mr^2 \quad . \tag{8-12}$$

Defining

$$x_1 = \theta \quad ,$$

$$x_2 = d\theta/dt \quad ,$$

$$a_1 = (g/r) \quad ,$$

$$a_2 = 1/mr^2 \quad ,$$

Eq. (8-12) can be written in state space form as

$$dx_1/dt = x_2 \quad , \tag{8-13}$$

$$dx_2/dt = -a_1\sin(x_1) + a_2T \quad . \tag{8-14}$$

8.2.2 The Hamilton-Jacobi Equation

Our goal now is to design a feedback control algorithm to regulate the robotic arm around a given position. Following the prescriptions from Sect. 8.1, first we define a cost function, then solve the associated Hamilton-Jacobi equation.

The efficiency of the final design depends fundamentally on the selection of the cost function. On the other hand, the analytic solution of the problem can be simplified by selecting an adequate cost function also. In this section we will show how two different cost functions lead to different results.

We first try a cost function that minimizes the position error and the acceleration. For simplicity we will assume that the desired position is $x_1 = 0$, Then,

$$J_1 = \int_0^{tf} [1/2\ (x_1)^2 Q + 1/2\ (dx_2/dt)^2 R]dt \quad . \tag{8-15}$$

The associated Hamiltonian will be

$$H_1 = w_1 x_2 + w_2(-a_1\sin(x_1)+a_2T)$$

$$+ 1/2\ (x_1)^2 Q + 1/2\ (-a_1\sin(x_1)+a_2T)^2 R \quad . \tag{8-16}$$

The optimal control must satisfy $H_u = 0$; therefore,

$$w_2 a_2 + a_2(-a_1\sin(x_1)+a_2T)R = 0 \quad . \tag{8-17}$$

Using Eq. (8-17) and demanding $H_1 = 0$, it follows that

$$0 = w_1 x_2 - (w_2)^2/2R + 1/2\ (x_1)^2 Q \quad . \tag{8-18}$$

Our goal is to obtain a solution that is independent of x_1 or x_2. Consider:

$$w_1 = p_{11}x_1 + p_{12}x_2 \quad ; \tag{8-19a}$$

$$w_2 = p_{12}x_1 + p_{22}x_2 \quad . \tag{8-19b}$$

By introducing Eq. (8-19) into Eq. (8-18) and performing some algebraic operations, we obtain:

$$0 = x_1 x_2(p_{11} - p_{12}p_{22}) \quad , \tag{8-20a}$$

$$0 = (x_1)^2(Q - (p_{12})^2/R) \quad , \tag{8-20b}$$

$$0 = (x_2)^2(p_{12} - (p_{22})^2/2R) \quad . \tag{8-20c}$$

We can now find a solution for Eq. (8-20) that is independent of the state (x_1 or x_2). Again, some algebraic manipulations lead to

$$p_{12} = (QR)^{1/2} \quad , \tag{8-21a}$$

$$p_{22} = (2R(QR)^{1/2})^{1/2} \quad , \tag{8-21b}$$

$$p_{11} = R(2Q(QR)^{1/2})^{1/2} \quad , \tag{8-21c}$$

which is the only real solution of Eq. (8-20).

From Eq. (8-17), we can obtain the optimal control as a function of x_1 and w_2. The quantity w_2 can be expressed now as a function of x_1 and x_2 using Eqs. (8-19) and (8-21). The optimal control can be, in this way, expressed in a closed-loop form as

$$T = (1/a_2)(a_1\sin(x_1) - (Q/R)^{1/2}x_2 - (2Q(QR)^{1/2})^{1/2}x_1) \quad . \tag{8-22}$$

Introducing optimal control into our model, we can perform stability analysis. The reader can easily check that this optimal control strategy is stable for any value of Q and R, but the system eigenvalues may have an imaginary part, depending on the gains we choose. To avoid this problem, we need to come back to the original cost function and reconsider our original formulation.

Considering the cost function, we realize that the velocity has not been minimized. Now we solve again the problem by introducing this extra requirement; that is, we try a cost function that minimizes the position error, the velocity error, and the acceleration. For simplicity we will assume that the desired position is $x_1 = 0$ and the desired velocity is $x_2 = 0$. Then,

$$J_1 = \int_0^T [1/2\ (x_1)^2Q_1 + 1/2\ (x_2)^{1/2}Q_2 + 1/2\ (dx_2/dt)^2R]dt \quad , \tag{8-23}$$

and the associated Hamiltonian will be

$$\begin{aligned} H_1 &= w_1x_2 + w_2(-a_1\sin(x_1)+a_2T) \\ &\quad + 1/2\ (x_1)^2Q_1 + 1/2\ (x_2)^{1/2}Q_2 + 1/2\ (-a_1\sin(x_1)+a_2T)^2R \quad . \end{aligned} \tag{8-24}$$

The optimal control must satisfy $H_u = 0$; therefore,

$$w_2a_2 + a_2(-a_1\sin(x_1)+a_2T)R = 0 \quad . \tag{8-25}$$

Using Eq. (8-25) and demanding that $H_1 = 0$, it follows that

$$0 = w_1x_2 - (w_2)^2/2R + 1/2\ (x_1)^2Q_1 + 1/2\ (x_2)^{1/2}Q_2 \quad . \tag{8-26}$$

Trying as before:

$$w_1 = p_{11}x_1 + p_{12}x_2 \quad , \qquad (8\text{-}27a)$$

$$w_2 = p_{12}x_1 + p_{22}x_2 \quad . \qquad (8\text{-}27b)$$

By introducing Eq. (8-27) into Eq. (8-26) and making some algebraic operations, we obtain

$$0 = x_1x_2(p_{11} - p_{12}p_{22}) \quad , \qquad (8\text{-}28a)$$

$$0 = (x_1)^2(Q_1 - (p_{12})^2/R) \quad , \qquad (8\text{-}28b)$$

$$0 = (x_2)^2(p_{12} - (p_{22})^2/2R + Q_2/2) \quad , \qquad (8\text{-}28c)$$

and

$$p_{12} = (Q_1R)^{\frac{1}{2}} \quad , \qquad (8\text{-}29a)$$

$$p_{22} = (2R(Q_1R)^{\frac{1}{2}}+Q_2R)^{\frac{1}{2}} \quad , \qquad (8\text{-}29b)$$

$$p_{11} = R(2Q_1(Q_1R)^{\frac{1}{2}}+Q_1Q_2)^{\frac{1}{2}} \quad , \qquad (8\text{-}29c)$$

which is the only real solution of Eq. (8-28). Now we have more freedom to adjust the eigenvalues in the desired position.

Finally, if we choose to minimize the velocity and the acceleration, then, for any value of Q and R, the eigenvalues are imaginary.

8.3 CONCLUSIONS

In this section, we have presented a detailed example of solving the Hamilton-Jacobi equation.

The fundamental advantages of this approach are that: (1) the system is stable for any selection of weights, and (2) the final implementation can be done using standard proportional integral-differential (PID) boxes and function generators. No differential equations are needed.

The main disadvantage of this approach is the substantial analytic work required when the systems are nonlinear. Some simplification can be obtained by redefining the cost function.

If the system is linear and our goal is to design a steady state regulator, then the Hamilton-Jacobi approach reduces to the well-known LQ algorithm.

9. A NEW APPROACH TO CONTROL THE WATER LEVEL OF U-TUBE STEAM GENERATORS

Automatic water level control in steam generators is currently achieved via the three-element controller. This algorithm is based on the measurements of level, steam flow, and feedwater flow. Unfortunately, at low power the feedwater flow signal is highly unreliable, forcing the transfer to manual control. A large number of reactor trips occur under these conditions. The nuclear industry has shown a concern for this problem.

In this section, an alternative automatic control algorithm is proposed and validated. The new algorithm does not rely on flow signals. Instead, it uses the pressure measurement in the steam header. A level set point modulation is introduced that allows the algorithm to compensate for the shrink and swell phenomena. The standard Δ-P algorithm to control feedwater pump speed has been also modified to achieve greater performance and integration.

9.1 STEAM GENERATOR DYNAMICS

The U-tube steam generator (SG) dynamics is very attractive from the mathematical point of view, but it is a nightmare for the plant operator. The SG dynamic behavior is characterized by strong nonlinearities at low power and by the so-called "nonminimum phase" problem. Both effects need to be compensated by the control designer.

Perturbations in pressure or enthalpy can put the water level and the water inventory in the SG out of phase for large periods (10 to 100 s). This might mean that for several seconds the amount of water introduced into the system is more than the amount of steam leaving it, and the level may be decreasing instead of increasing. This change can affect dramatically the controllability of the system and must be taken into account.

Out-of-phase perturbations can be introduced by changes in (1) steam flow, (2) primary enthalpy, or (3) feedwater enthalpy. These phenomena are called nonminimum phase or shrink and swell problems.

On the other hand, the strong nonlinearities present in the system can also affect our design. If the system is linearized, one can get the impression of having a stable model. The system can be stable, actually, only under small perturbations. A large perturbation will make it unstable. This effect is more evident at low power, and it seems to be the most important source of failure in control designs.

9.2 EXISTING CONTROLLERS

This section reviews control options available to date to the nuclear industry.

9.2.1 One-Element Controller

A minimization of the level error using a standard PID box leads to the one-element controller. Because of the out-of-phase period, this design can lead to instabilities.

Based on this approach, some naive designs have been proposed for low-power operation. These designs calculate the gains for the PID level controller based on a linearized model. The linearized model may give the (wrong) impression of a stable system. Even if this were true, the PID gains would be so small that the system would respond too slowly to the usual power ramps.

9.2.2 Three-Element Controller

Figure 9.1 shows a block diagram of a three-element controller. Now, not only the level error is minimized, but also the difference between the steam and feedwater flows. In this way, the out-of-phase periods are, in some way, compensated. This design is highly effective. Unfortunately, at low power the feedwater flow signal is unreliable; therefore, the three-element controller cannot be used.

9.2.3 The Belgian Level Controller

Belgian nuclear power plants use an automatic feedwater control that can perform under any operating conditions.[12] It is based on an adaptive three-element design that includes a shrink and swell compensator. At low power, the feedwater flow becomes unreliable. The Belgian design solves this problem by using a one-element controller with a new shrink and swell compensator.

The compensators for low power and for full power are different. At full power the steam flow signal is used, and at low power the wide range level signal is used. We have been unable to get detailed information on how the signals really work, but the operational experience seems to be satisfactory.

9.3 LEVEL SET POINT MODULATION

This section presents a novel algorithm to control the water level automatically under any operating conditions. The algorithm is based on the one-element controller, but it uses a level set point modulation technique to compensate for out-of-phase phenomena.

First, the model used to perform the steam generator simulation is presented. Then, the SG dynamics under the action of the one-element controller is studied. It is shown how the gains needed to follow the

• **Minimizes level error and flow difference**

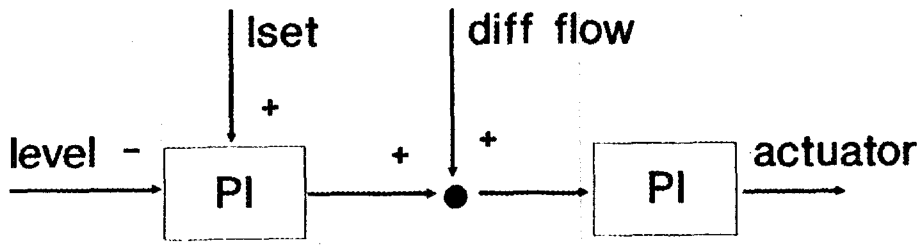

Fig. 9.1. Diagram of a three-element controller.

standard power ramps are too big and can make the system unstable at low power. Finally, a level set modulation technique able to compensate for the nonminimum phase phenomenon is formulated and validated.

9.3.1 Steam Generator Model

The MMS library[13] has been used to develop the SG model. The modules used represent the

1. feedwater pump (including turbine and turbine valve),
2. main feedwater valve and actuator,
3. U-tube steam generator, and
4. connectors and pipes.

The parameters used for this model are taken from a Combustion Engineering PWR (Arkansas Nuclear One).

Figure 9.2 gives a graphical representation of the level scales in this SG.

9.3.2 One-Element Controller Dynamics

Using the standard PID boxes of the MMS library, a one-element controller was added to the model. A power ramp of 0.05%/s was simulated.

The PID box was adjusted to keep the level near the set point during the transient. Figure 9.3 graphically represents the results.

To keep the level error small, it was necessary to have strong gains. The power ramp used is the one required by the nuclear industry for its level control algorithms.

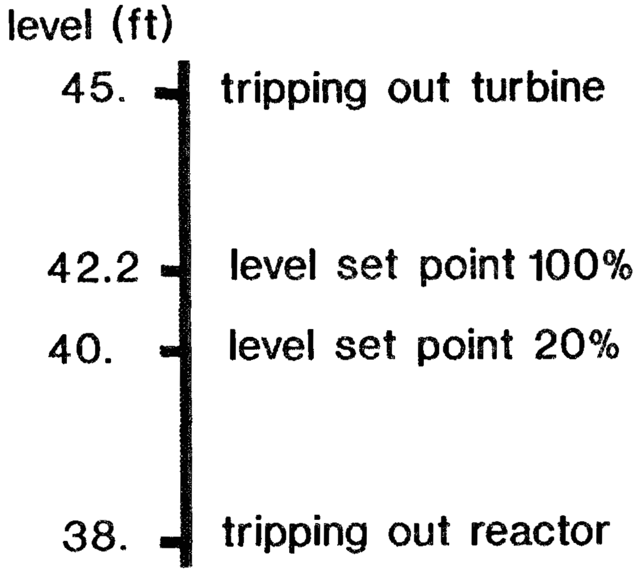

Fig. 9.2. Steam generator level scale.

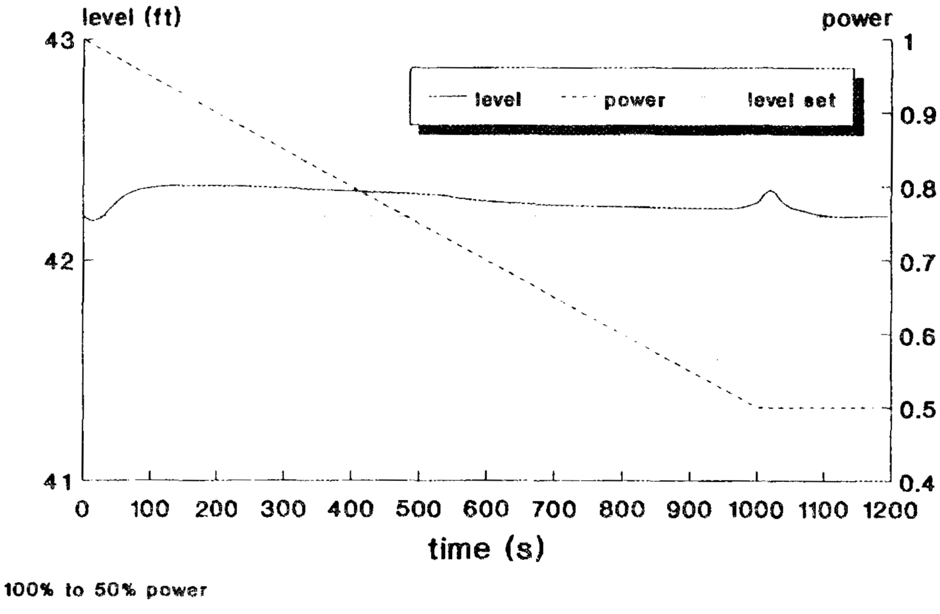

Fig. 9.3. Steam generator response to a power ramp.

A strong gain keeps the level near the set point, but it also can make the system unstable. Figure 9.4 shows the results of a step change in steam flow at 100% power. If the steam flow is reduced, the pressure of the steam increases, inducing a contraction of the steam bubbles in the water. The level controller is acting in the opposite direction. The feedwater flow is increasing when the steam flow has been reduced for a period of about 30 s. This out-of-phase period will produce a large overshoot.

The results are catastrophic at low power. Figure 9.5 presents a simulation of a step change in steam flow at 25% power. Although this time the step is smaller in absolute value, the system becomes unstable. Moreover, the instability has a nonlinear nature. The linearization around the set point, however, will make us believe that the system was stable.

9.3.3 Level Set Point Modulation

We have seen that the gains necessary to follow a power ramp are too large and that the SG may become instable. This instability is mainly induced by the out-of-phase phenomenon. The level can be decreasing while the water inventory is increasing. It is necessary to compensate in some way the level controller if a large perturbation is introduced into the system.

We have introduced a level set modulation technique to avoid these problems. We define $Lset_0$ as the desired level set point. In our algorithm, the actual level set point sent to the one-element controller will be $Lset$, defined as:

$$Lset = Lset_0 + L_p \quad , \tag{9-1}$$

where L_p is a modulated correction factor that we obtain from

$$dL_p/dt = -L_p/\tau_p - K_p(dP/dt) \quad , \tag{9-2}$$

where P is the pressure signal, and K_p and τ_p are positive gains to be adjusted by the control designer.

9.3.4 Simulation Results

The level set modulation technique was implemented on the MMS steam generator model. A standard PID box was used for the one-element controller. The pressure signal was filtered before taking the numerical derivative. The derivative was filtered again through a band limiter, because we are interested only in compensating for large perturbations.

Figure 9.6 graphically displays the simulation results at 100% power. Figure 9.7 compares the dynamic behavior of the system (1) without level modulation and (2) with level modulation.

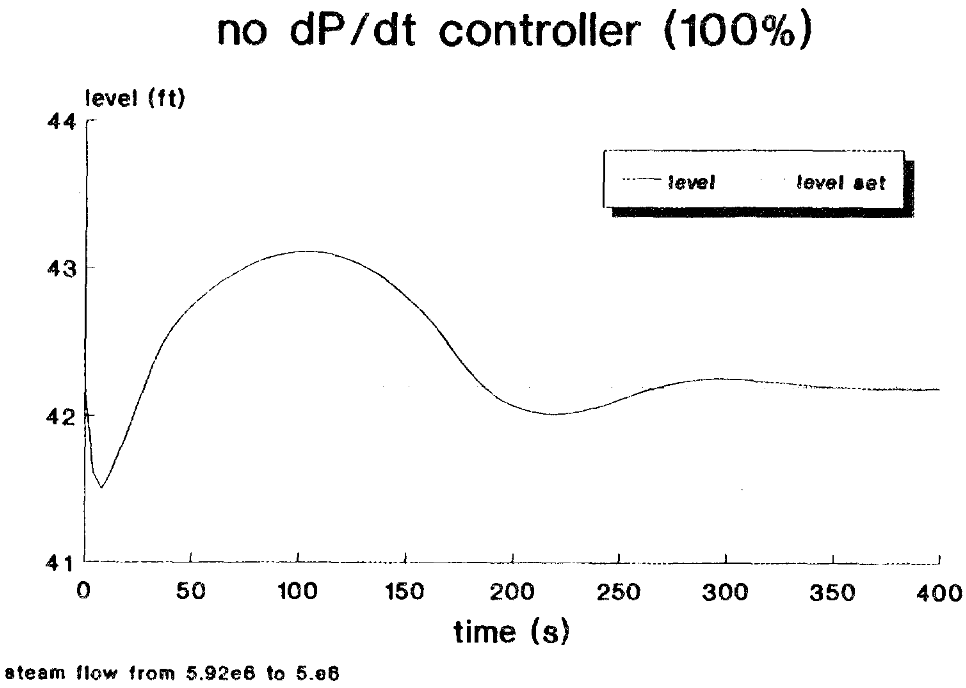

Fig. 9.4. Steam generator response to a steam flow step perturbation: 100% power.

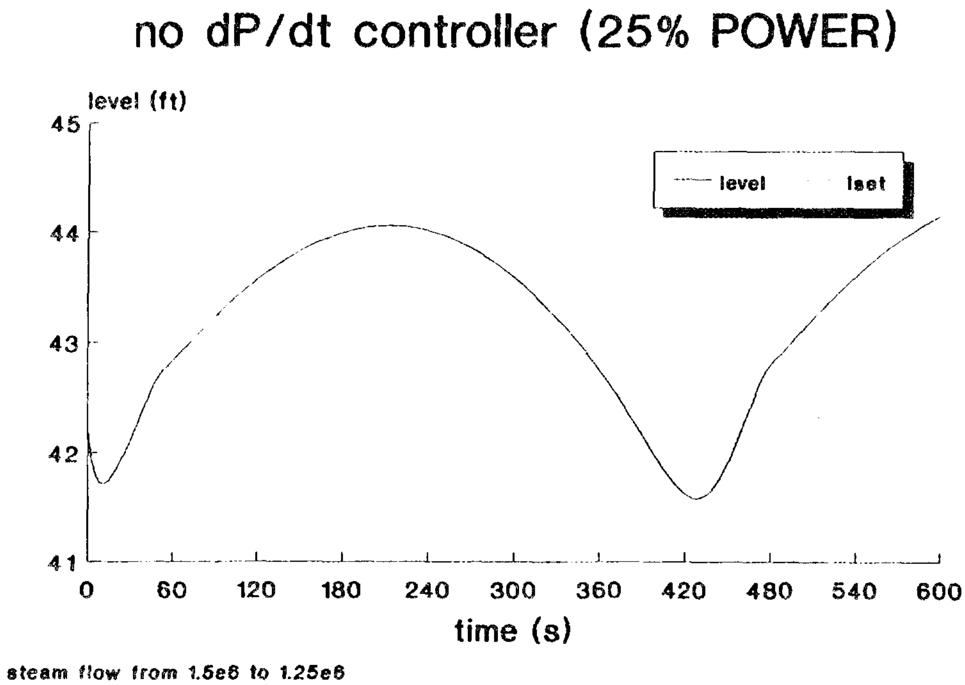

Fig. 9.5. Steam generator response to a steam flow step perturbation: 25% power.

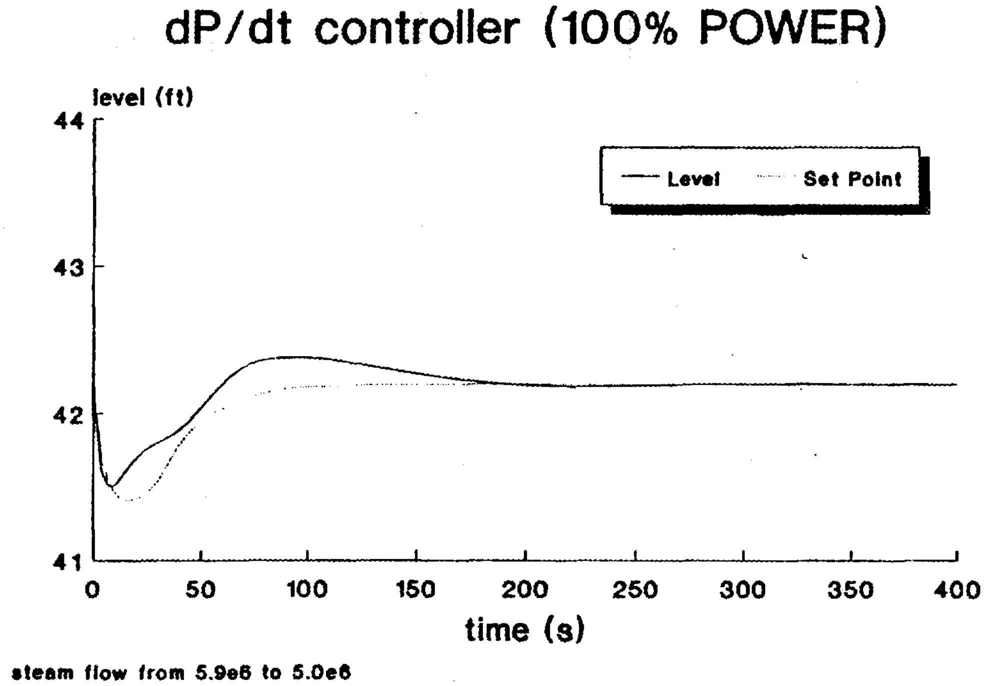

Fig. 9.6. Steam generator level response to a steam flow step perturbation: 100% power, level modulation on.

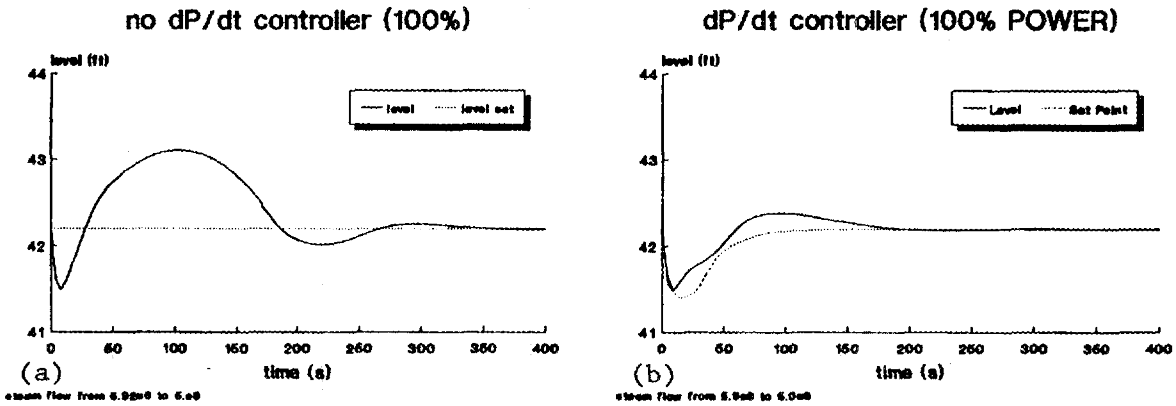

Fig. 9.7. Comparison steam generator response, 100% power: (a) level modulation off and (b) level modulation on.

The effect of the compensation is more dramatic at low power. Figure 9.8 presents the simulation results at 25% power, and Fig. 9.9 compares them with the ones obtained without modulation.

9.4 PUMP SPEED CONTROLLER

The pump speed is controlled using the Δ-P algorithm. The idea is to operate the pump in such a way that the difference in pressure between the steam header and the pump exit is almost constant. The problem in this design will be that the pump speed controller does not use the level error information; therefore, in some special scenarios, it can act against the level controller.

In our design, we have changed the control concept for the pumps. Two factors will contribute to the controller, (1) a valve set program and (2) the level error.

Figure 9.10 is a diagram of the valve set program. Given a steam flow signal (a power signal could also be used), a function generator returns the optimal valve position. This function generator has been designed off-line so as to optimize the position of the valve to ensure a nice difference of pressure and a safe controllability margin.

The optimal valve position signal is then filtered to introduce a delay (in this design, the delay was 30 s). This delay must be introduced to avoid abrupt reactions on the controller.

The filter signal is then added to the one-element controller signal and sent to the feedwater valve. Simultaneously, the error between the actual position of the feedwater valve and the desired position is added to the one-element controller signal and sent to an integral box that actuates the pump valve.

Figure 9.11 gives the diagram for the integrated control algorithm: level modulator, one-element controller, and valve set program.

Figure 9.12 shows the positions of the feedwater and pump valves during the simulated 100% power transient. The behavior of the integrated controller is clear. The fast proportional information is sent to the feedwater valve, while the pump valve executes a slow integral movement to correct for steady state errors and to make the feedwater valve move to the optimal position.

9.5 FUTURE WORK

The algorithm presented in this chapter is ready to be implemented in any operating steam generator. The design was based on the capabilities of the Foxboro hardware and, therefore, no new hardware development will be necessary.

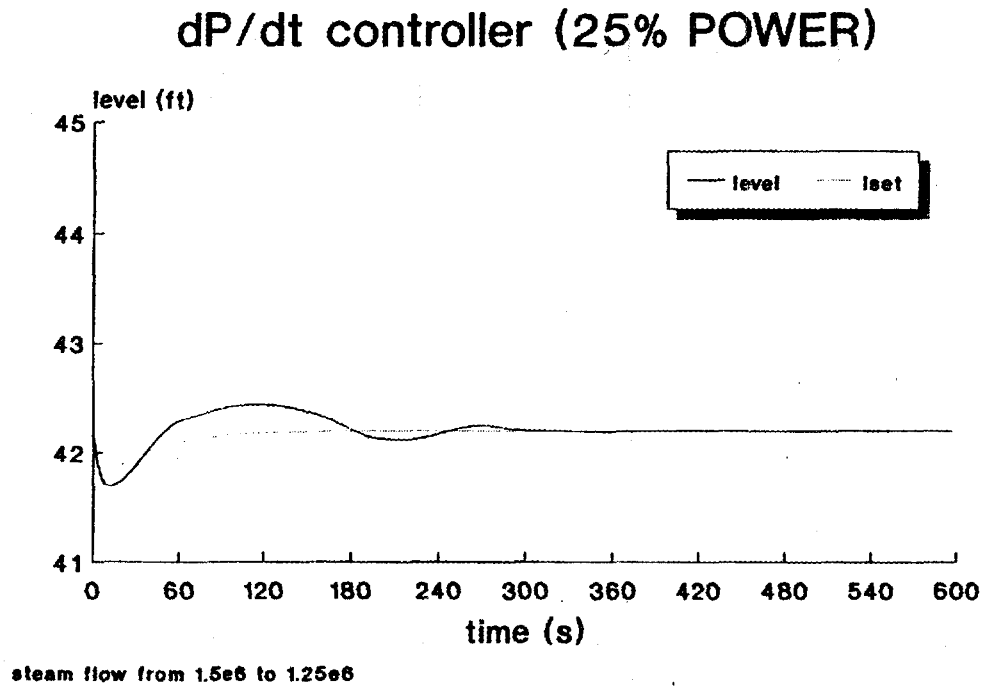

Fig. 9.8. Steam generator level response to a steam flow step perturbation: 25% power, level modulation on.

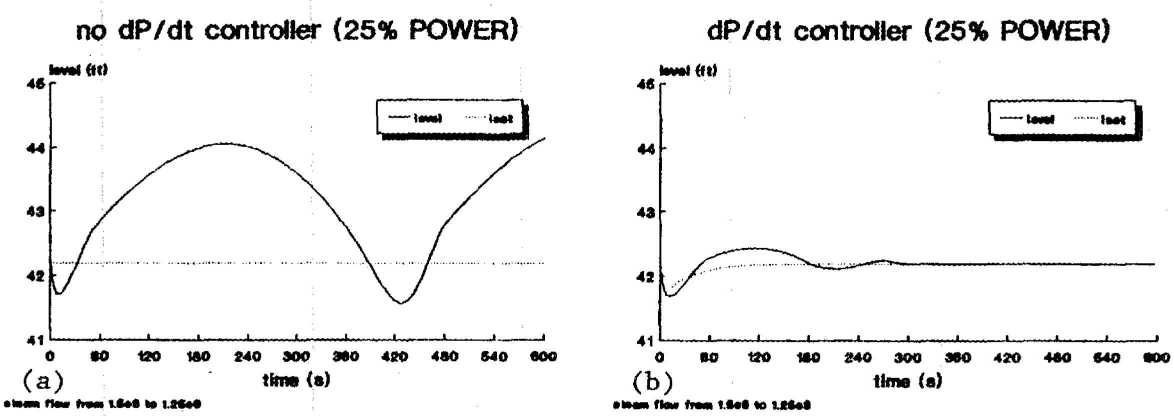

Fig. 9.9. Comparison of steam generator response: 25% power: (a) level modulation off and (b) level modulation on.

- A valve set program is introduced that substitutes the delta-P controller

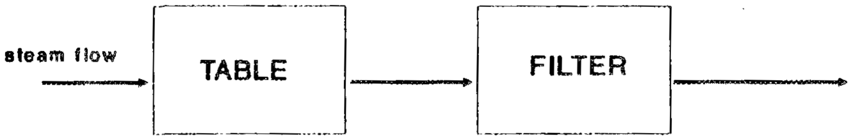

Fig. 9.10. Diagram of the valve set program.

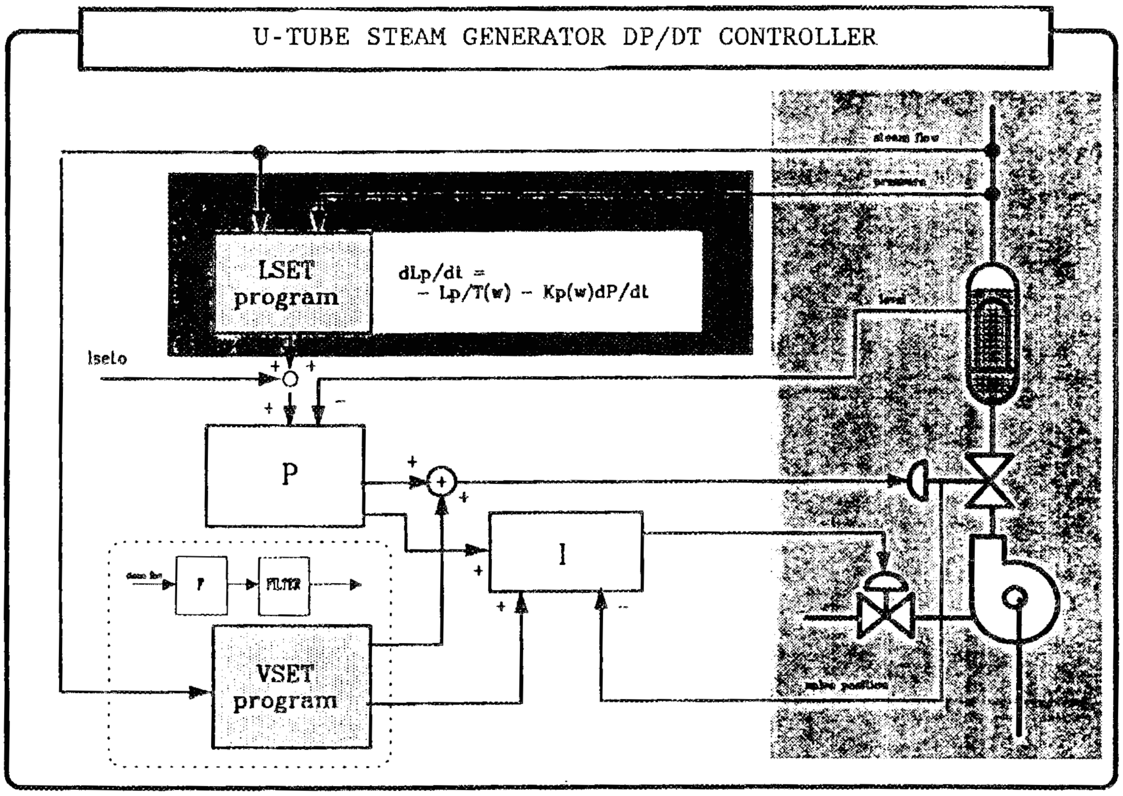

Fig. 9.11. Diagram of the integrated control system.

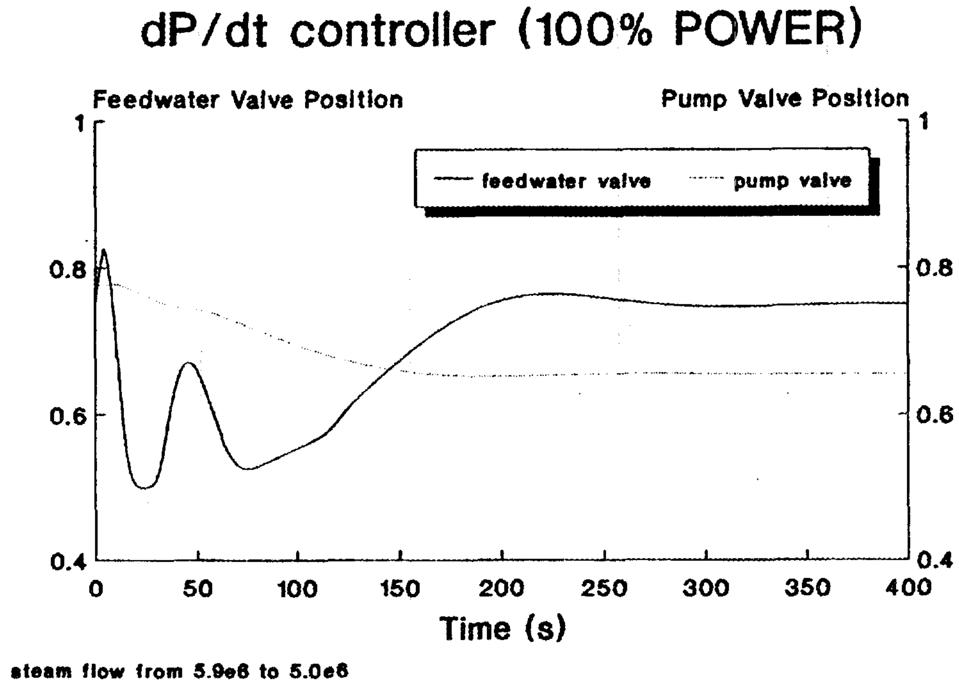

Fig. 9.12. Steam generator valve positions during a transient.

We think that the capabilities of the algorithm could be enhanced by taking into account feedwater and primary enthalpy perturbations. Both perturbations introduce an out-of-phase period into the system that can be compensated by using again the level modulation technique. Let L_p, L_{tp}, and L_{tf} represent the modulated corrections for pressure, primary temperature, and feedwater temperature. The modulated level set point signal sent to the one-element controller will be given by

$$Lset = Lset_0 + L_p + L_{tp} + L_{tf} \quad , \tag{9-3}$$

$$dL_p/dt = -L_p/\tau_p - K_p(dP/dt) \quad , \tag{9-4}$$

$$dL_{tp}/dt = -L_{tp}/\tau_{tp} + K_{tp}(dT_p/dt) \quad , \tag{9-5}$$

$$dL_{tf}/dt = -L_{tf}/\tau_{tf} - K_{tf}(dT_f/dt) \quad , \tag{9-6}$$

where T_p and T_f represent the primary and secondary temperature signals.

On the other hand, it will also be interesting to study the effects induced by the coupling of more than one steam generator connected to the same feedwater line. In this case, perhaps the original Δ-P controller will perform better than the proposed valve set program because, by keeping the pressure difference constant, it will be possible to minimize the coupling effects.

Finally, better simulation of real low power is needed. The MMS model used in this work failed at very low power. It will be necessary to use the extended range modules of the MMS library.

9.6 SUMMARY

In this section, an alternative automatic control algorithm has been proposed. The new algorithm does not rely on flow signals. Instead, it uses the pressure measurement in the steam header. A level set point modulation is introduced that allows the algorithm to compensate for the shrink and swell phenomenon. The standard Δ-P algorithm to control feedwater pump speed has also been modified to achieve greater performance and integration.

The algorithm has been validated using a detailed U-tube steam generator model based on the MMS library.

10. CONCLUSIONS

This report has studied, developed, and validated advanced control techniques for nuclear reactors and mechanical manipulators.

The nuclear industry is now in the process of moving to digital hardware. Because of this unique opportunity to update the actual control algorithms, there is a generalized interest in knowing the benefits of applying new advanced control techniques to nuclear plants. The research presented in this report is a contribution to that knowledge.

The optimal control theory has been analyzed from a stability point of view. It has been found that the classical formulation of Pontryagin leads to open-loop strategies, and that the alternative formulation which leads to stable closed-loop implementations, the so-called LQ algorithm, can be applied only to linear systems.

Unfortunately, real-life systems are seldom linear, and if linear, rarely exact models of the plants available. Even if we had an exact model, a large number of differential equations would be involved, making the computation of advanced control strategies impossible. The main effort of this report has been to develop the necessary theory to simplify all these problems.

First, the basic relationship between Pontryagin's optimal control theory and the alternative Kalman's LQ algorithm has been identified.

Based on this study, new algorithms have been proposed that are able to deal directly with nonlinear models, to track time-varying parameters or uncertainties, to decompose large models into a set of decoupled submodels, and to handle noisy signals.

These new techniques have been validated with a large number of examples. Applications to PWRs, BWRs, ANS, steam generators, and mechanical manipulators have been simulated in digital computers, and the results have been published in nine peer-reviewed papers.[14,15,16,17,18,19,20,21,22]

10.1 ACCOMPLISHMENTS

The main accomplishments of this research can be summarized as follows.

10.1.1 Closed-Loop Optimal Control

In Sect. 2, the basic relationship between optimal control theory and closed-loop control design is identified. The purpose of this work has been to show how the basic cost function minimization problem must be reformulated to obtain a closed-loop control strategy. New approaches to this problem that are able to handle directly nonlinear models have been developed. Some new applications of the closed-loop optimal control theory have been proposed: state estimation, parameter tracking, uncertainty tracking, and system decomposition.

10.1.2 Parameter Tracking

Section 3 presents a new formulation of a class of nonlinear optimal control problems in which system parameters change arbitrarily with time. The methodology has been validated with a PWR model.

10.1.3 State Estimation and Filtering

Section 4 presents a new formulation of a class of nonlinear optimal control problems in which system signals are noisy and some system parameters change arbitrarily with time. The methodology has been validated with an application to a nonlinear PWR model.

10.1.4 Plant Monitoring

Section 5 shows some applications of the techniques presented in this report to the reactor monitoring problem. First, a transient reactivity monitor has been presented, which was tested and validated with a dynamic model of the ANS. Second, a state monitor for a PWR has been presented that is able to estimate the state variables of the system by analyzing the noise-corrupted signals from the plant. Both applications use techniques presented in previous sections.

10.1.5 Comparison of PI and Optimal Controllers

Section 6 presents a comparison of the behavior of a BWR controlled with a standard PI controller and a BWR controlled with a microprocessor-based optimal control algorithm.

10.1.6 Uncertainty Tracking and Large System Decoupling

Section 7 presents an adaptive optimal control algorithm for uncertain nonlinear systems. It represents a novel approach to the problem of decoupling a large system into a set of simplified subsystems. A variational technique based on Pontryagin's Maximum Principle has been used to track the system's unknown terms, decouple the subsystem models, and calculate the optimal control. To validate the algorithm, a system representing a two-link mechanical manipulator was simulated. The inverse kinematics problem for the trajectory prescription in generalized coordinates was also solved by applying optimal control techniques.

10.1.7 Applicability of the Hamilton-Jacobi Approach

Section 8 presents an application of the Hamilton-Jacobi approach to the mechanical manipulator problem.

10.1.8 Demand Modulation: SG Automatic Level Control

Section 9 presents a new algorithm to control steam generator water level that does not rely on feedwater flow measurements. At low power, the feedwater signal is biased; therefore, the classic three-element controller fails, forcing the transfer to manual operation. Manual operation has not been very effective; in fact, a substantial number of reactor trips occur under low-power manual operation. The new algorithm presented was able to compensate for the shrink and swell phenomenon by modulating the level set point according to differential changes on the pressure signals. In this manner, it was possible to keep a strong and dynamic automatic level controller from 0% to 100% power.

10.2 COMMENTS ABOUT SOME ALTERNATIVE APPROACHES

This report has been oriented to the study of the applicability of variational techniques to the advanced control design problem. Unfortunately, other powerful approaches, such as adaptive PID, self-tuning control, and robust control, have not been analyzed. These algorithms might be really efficient. They have the advantage of being easier to implement. It is important to understand that the main objective of advanced control algorithms is to improve the ratio between benefits and cost for the nuclear industry; therefore, the implementation cost should be taken into account when new algorithms are proposed.

On the other hand, simplicity can increase reliability. Each day, more powerful computers are becoming available. There are now personal computers able to perform computations at rates faster than 8 MIPS (mega instructions per second) and 2 MFLOPS (mega floating point calculations per second). These rates can lead us to the conclusion that we can create very sophisticated algorithms working in real time.

But, by increasing the necessary computational steps, we also increase the failure rate. Given the large safety margin required for nuclear reactors and the huge cost of downtime, simplicity should have an important weight factor in our future decisions.

REFERENCES

1. Z. R. Rosztoczy et al., "Application of the Pontryagin's Maximum Principle to Flux-State Changes in Nuclear Reactors," Proc. Reactor Kinetics and Control, University of Arizona, March 25-27, 1963.

2. L. S. Pontryagin et al., *The Mathematical Theory of Optimal Processes*, Trans. by K. N. Trirogoff, ed. by L. W. Neustadt, Wiley-Interscience, New York, 1962.

3. R. R. Mohler and C. N. Shen, *Optimal Control of Nuclear Reactors*, Academic Press, New York, 1970.

4. R. Hocepied et al., "Automatic Control of Water Level of Steam Generators from 0% to 100% of Load," *Nuclear Energy* 2, 133-142 (1978).

5. J. D. White, *Advance Control Program Plan for Advanced Reactors*, DOE/OR-894, U.S. DOE Oak Ridge Operations Offices, 1988.

6. D. G. Luenberger, *Introduction to Dynamic Systems*, Wiley, New York, 1979.

7. R. E. Kalman, "Contributions to the Theory of Optimal Control," *Boletin De La Sociedad Matematica Mexicana*, 102-109 (1960).

8. "Challenges to Control: A Collective View," *IEEE Trans. Automatic Control* **AC-32**(4) (1987).

9. R. D. Cheverton and T. M. Sims, *HFIR Core Nuclear Design*, Oak Ridge National Laboratory, Oak Ridge, Tennessee, ORNL-4621, July 1971.

10. C. D. West et al., *Center for Neutron Research Project Status Report*, Oak Ridge National Laboratory, Oak Ridge, Tennessee, ORNL/TM-10065, September 1986.

11. José March-Leuba, "A Reduced Order Model of Boiling Water Reactor Dynamics," *Nuclear Technology* **75**, 15-22 (October 1986).

12. R. Bayens, *The Belgian PWR Steam Generator Level Control System from Criticality to Full Power*, LABORELEC M02-87-052/R-RB-Mo, Belgium, 1987.

13. Babcock & Wilcox Company, *Modular Modeling System (MMS): A Code for the Dynamic Simulation of Fossil and Nuclear Power Plants*, March 1985.

14. J. March-Leuba and C. March-Leuba, "A Transient Reactivity Monitor Based on Optimal Control Theory," IEEE 1988 Nuclear Science Symposium, Orlando, Florida, November 1988.

15. C. March-Leuba, J. March-Leuba, and R. B. Perez, "Optimal Filtering, Parameter Tracking and Control of Nonlinear Nuclear Reactors," 1988 International Reactor Physics Conference, Jackson Hole, Wyoming, September 1988.

16. C. March-Leuba and R. B. Perez, *Optimal Control Theory of Load-Following and Parameter-Tracking of Nonlinear Systems: An Application of Pontryagin Maximum Principle to Reactor Dynamics*, Oak Ridge National Laboratory, Oak Ridge, Tennessee, ORNL/TM-10662, December 1987.

17. L. A. Rovere, P. J. Otaduy, and C. March-Leuba, "Development of an Uncertain Model Based Nonlinear Optimal Pressure Control System for a Nuclear Reactor," IEEE 1988 Nuclear Science Symposium, Orlando, Florida, November 1988.

18. C. March-Leuba and J. March-Leuba, "An Adaptive Nonlinear Filtering Algorithm for Optimal State Estimation of Nonlinear Nuclear Reactors," IEEE 1988 Nuclear Science Symposium, Orlando, Florida, November 1988.

19. C. March-Leuba and R. B. Perez, "Optimal Control of Nonlinear Nuclear Reactors," *Trans. Am. Nucl. Soc.* **55**, 617 (November 1987).

20. C. March-Leuba and R. B. Perez, "Optimal Control of Uncertain Nonlinear Systems: An Application to a Two-Link Robotic Arm," 1988 Control and Decision Conference, Knowledge-Based, Microprocessor-Implemented Session, December 1988.

21. C. March-Leuba and R. B. Perez, *Adaptive Optimal Control of Uncertain Nonlinear Systems: On-Line Microprocessor-Based Algorithm to Control Mechanical Manipulators*, Oak Ridge National Laboratory, ORNL/TM-10764, May 1988.

22. C. March-Leuba and R. B. Perez, "Adaptive Optimal Control of Uncertain Nonlinear Systems: On-line Microprocessor-Based Algorithm to Control Mechanical Manipulators," submitted to *J. Robotic Systems*, 1988.

INTERNAL DISTRIBUTION

1. S. J. Ball
2. R. S. Booth
3. H. R. Brashear
4. C. R. Brittain
5. N. E. Clapp
6. G. Desaussure
7. F. C. Difilippo
8. B. G. Eads
9. C. E. Ford
10. D. N. Fry
11. W. R. Hamel
12. F. J. Homan
13. J. K. Jones, Jr.
14. R. A. Kisner
15. H. E. Knee
16. R. C. Mann
17-26. C. March-Leuba
27. J. March-Leuba
28. D. W. McDonald
29. D. R. Miller
30. O. B. Morgan
31. J. K. Munro
32. F. R. Mynatt
33. L. C. Oakes
34. P. J. Otaduy
35. J. T. Robinson
36. R. L. Shepard
37. H. E. Trammell
38. R. E. Uhrig
39. C. R. Weisbin
40. J. D. White
41. T. L. Wilson
42. R. T. Wood
43. J. B. Ball, Advisor
44. P. F. McCrea, Advisor
45. T. B. Sheridan, Advisor
46-47. Central Research Library
48. Y-12 Technical Reference Section
49-50. Laboratory Records Department
51. Laboratory Records ORNL-RC
52. ORNL Patent Section
53. I&C Division Publications Office

EXTERNAL DISTRIBUTION

54. Assistant Manager for Energy Research and Development, U.S. Department of Energy, Oak Ridge Operations Office, Oak Ridge, TN 37831.
55. G. Santos-Leon, Energy Programs Division, U.S. Department of Energy, Oak Ride Operations Office, P.O. Box E, Oak Ridge, TN 37831.
56. H. Alter, Division of Advanced Technology Development, NE-462, U.S. Department of Energy, Washington, DC 20545.
57. J. I. Sackett, Argonne National Laboratory, 9700 South Cass Avenue, Argonne, IL 60439.
58. Y. Dayal, General Electric Company, Nuclear Systems Technology Operation, P.O. Box 530954, San Jose, CA 95153-5354.
59. T. W. Kerlin, The University of Tennessee, Department of Nuclear Engineering, 315 Pasqua Building, Knoxville, TN 37996.
60. B. R. Upadhyaya, The University of Tennessee, Department of Nuclear Engineering, 315 Pasqua Building, Knoxville, TN 37996.
61. R. Perez, The University of Tennessee, Department of Nuclear Engineering, 315 Pasqua Building, Knoxville, TN 37996.
62. M. Bailey, The University of Tennessee, Department of Electrical and Computer Engineering, Knoxville, TN 37996-2100.

63. M. Jamshidi, University of New Mexico, Department of Electrical and Computer Engineering, Albuquerque, NM 87131.
64. J. Bernard, Massachusetts Institute of Technology, Department of Nuclear Engineering, 77 Massachusetts Avenue, Cambridge, MA 02139.
65. Dr. José March España, Albacete 3-7, Valencia 46007, Spain.
66. Dr. Fernando Senent, Universidad de Valencia, Facultad de Ciencias Fisicas, Departamento de Fisica Atomica, Valencia, Spain.
67. Dr. Bolta, Universidad de Valencia, Facultad de Ciencias Fisicas, Departamento de Fisica Atomica, Valencia, Spain.
68. Dr. Peregrin Olcina, Universidad de Valencia, Facultad de Ciencias Fisicas, Departamento de Fisica Atomica, Valencia, Spain.
69. Dr. Ferrer Soria, Universidad de Valencia, Facultad de Ciencias Fisicas, Departamento de Fisica Atomica, Valencia, Spain.
70. Dr. Diaz Medina, Universidad de Valencia, Facultad de Ciencias Fisicas, Departamento de Fisica Atomica, Valencia, Spain.
71. Dr. Ferrero Calabuig, Universidad de Valencia, Facultad de Ciencias Fisicas, Departamento de Fisica Atomica, Valencia, Spain.

72-81. Office of Scientific and Technical Information, P.O. Box 62, Oak Ridge, TN 37831.